

Design and Analysis of a Three Degrees of Freedom (DOF) Parallel Manipulator with Decoupled Motions

by

Jijie Qian

A Thesis Submitted in Partial Fulfillment
of the Requirements for the Degree of

Master of Applied Science

in

The Faculty of Engineering and Applied Science

Mechanical Engineering

University of Ontario Institute of Technology

April 2009

© Jijie Qian, 2009

CERTIFICATE OF APPROVAL

Submitted by: Jijie Qian

Student #: 100333621

In partial fulfillment of the requirements for the degree of:

Master of Applied Science in Mechanical Engineering

Date of Defense (if applicable): April 7, 2009

Thesis Title:

Design and Analysis of a Three Degrees of Freedom (DOF) Parallel Manipulator with Decoupled Motions

The undersigned certify that they recommend this thesis to the Office of Graduate Studies for acceptance:

Chair of Examining Committee Signature Date (yyyy/mm/dd)

External Examiner Signature Date (yyyy/mm/dd)

Member of Examining Committee Signature Date (yyyy/mm/dd)

Member of Examining Committee Signature Date (yyyy/mm/dd)

As research supervisor for the above student, I certify that I have read the following defended thesis, have approved changes required by the final examiners, and recommend it to the Office of Graduate Studies for acceptance:

Prof. Dan Zhang _____
Name of Research Supervisor Signature of Research Supervisor Date (yyyy/mm/dd)

Abstract

Parallel manipulators have been the subject of study of much robotic research during the past three decades. A parallel manipulator typically consists of a moving platform that is connected to a fixed base by at least two kinematic chains in parallel. Parallel manipulators can provide several attractive advantages over their serial counterpart in terms of high stiffness, high accuracy, and low inertia, which enable them to become viable alternatives for wide applications. But parallel manipulators also have some disadvantages, such as complex forward kinematics, small workspace, complicated structures, and a high cost. To overcome the above shortcomings, progress on the development of parallel manipulators with less than 6-DOF has been accelerated.

However, most of presented parallel manipulators have coupled motion between the position and orientation of the end-effector. Therefore, the kinematic model is complex and the manipulator is difficult to control.

Only recently, research on parallel manipulators with less than six degrees of freedom has been leaning toward the decoupling of the position and orientation of the end-effector, and this has really interested scientists in the area of parallel robotics. Kinematic decoupling for a parallel manipulator is that one motion of the up-platform only corresponds to input of one leg or one group of legs. And the input cannot produce other motions.

Nevertheless, to date, the number of real applications of decoupled motion actuated parallel manipulators is still quite limited. This is partially because effective development strategies of such types of closed-loop structures are not so obvious. In

addition, it is very difficult to design mechanisms with complete decoupling, but it is possible for fewer DOF parallel manipulators. To realize kinematic decoupling, the parallel manipulators are needed to possess special structures; therefore, investigating a parallel manipulator with decoupling motion remains a challenging task.

This thesis deals with lower mobility parallel manipulator with decoupled motions. A novel parallel manipulator is proposed in this thesis. The manipulator consists of a moving platform that is connecting to a fixed base by three legs. Each leg is made of one C (cylinder), one R (revolute) and one U (universal) joints. The mobility of the manipulator and structure of the inactive joint are analyzed. Kinematics of the manipulator including inverse and forward kinematics, velocity equation, kinematic singularities, and stiffness are studied. The workspace of the parallel manipulator is examined. A design optimization is conducted with the prescribed workspace.

It has been found that due to the special arrangement of the legs and joints, this parallel manipulator performs three translational degrees of freedom with decoupled motions, and is fully isotropic. This advantage has great potential for machine tools and Coordinate Measuring Machine (CMM).

Keywords

Parallel manipulator; Decoupled motion; Screw theory; Isotropy; Inverse kinematic; Forward kinematic; Jacobian; Singularity; Stiffness; Workspace; Optimization.

Dedication

To my wife Ying, my daughter Casey and my parents.

Acknowledgments

First, I would like to express my deepest gratitude to my supervisor, Professor Dan Zhang, for his invaluable supervision, for suggesting the topic of this work, providing continuous guidance, support and encouragement throughout the research and critical review of the manuscript.

I am grateful to Professor Ebrahim Esmailzadeh and Professor Xiaodong Lin for their contributions as my Master thesis defense committee members.

I would like to thank all my colleagues in the Robotics and Automation Laboratory for their help and cooperation.

I am deeply indebted to my parents for their love, patience and support.

In addition, finally, I am greatly indebted to my wife Ying and my daughter Casey, for their love and support, for being my courage and my guiding light.

Thank you all from the bottom of my heart!

Table of Contents

Title Page.....	i
Abstract.....	iii
Keywords.....	iv
Dedication.....	v
Acknowledgements.....	vi
Table of Contents.....	vii
List of Tables.....	x
List of Figures.....	xi

Chapters

1. Introduction.....	1
1.1 History of Robots.....	1
1.2 Robotic Architectures.....	8
1.2.1 Serial Architecture.....	9
1.2.2 Parallel Architecture.....	10
1.2.3 Hybrid Architecture.....	12
1.3 Fully Parallel and Non-fully Parallel Manipulator.....	13
1.4 Summary of the Developed Robot.....	15
2. Conceptual Design.....	19
2.1 Introduction.....	19
2.1.1 Classification of Kinematic Decoupling.....	19
2.1.2 Isotropy.....	21

2.1.3	Screw Theory and Mobility Analysis.....	24
2.1.4	Over-Constrained Parallel Manipulator.....	33
2.2	Geometrical Design.....	34
2.3	Mobility Analysis of the Manipulator.....	38
2.4	Inactive Joint.....	39
3.	Kinematic Modeling of the 3-CRU Parallel Manipulator.....	41
3.1	Introduction.....	41
3.2	Inverse Kinematics.....	42
3.3	Forward Kinematics.....	45
3.4	Velocity Analysis.....	45
3.5	Singularity Analysis.....	46
3.5.1	Constraint Singularity.....	46
3.5.2	Kinematic Singularity.....	47
3.6	Stiffness Analysis.....	48
3.6.1	Introduction.....	48
3.6.2	General Stiffness Model for Parallel Manipulator.....	49
3.6.3	Stiffness Mapping.....	50
4.	Workspace Analysis and Prototype Design.....	55
4.1	Definition of Workspace.....	55
4.2	Workspace Analysis of the 3-CRU Parallel Manipulator.....	56
4.3	Prototype Design.....	57
5.	Design Optimization.....	59
5.1	Introduction.....	59

5.2	Genetic Algorithms.....	60
5.3	The Optimum Design of the 3-CRU Parallel Manipulator with Prescribed Workspace.....	62
6.	Conclusions and Future Research.....	68
6.1	Conclusions.....	68
6.2	Major Contributions.....	69
6.3	Future Research.....	70
	Reference.....	71

List of Tables

Table 1.1 Comparison between Serial and Parallel manipulator.....	14
Table 2.1 Reciprocal conditions for two screws.....	26
Table 3.1 Stiffness in X vs. stiffness of actuators.....	51
Table 3.1 Stiffness in Y vs. stiffness of actuators.....	51
Table 3.1 Stiffness in Z vs. stiffness of actuators.....	51
Table 5.1 Original design parameters and optimum design parameters.....	67

List of Figures

Figure 1.1 The first spatial industrial parallel robot.....	2
Figure 1.2 The first octahedral hexapod or the original Gough.....	3
Figure 1.3 The flight simulator of Klaus Cappel, based on an octahedral hexapod.....	4
Figure 1.4 Schematic drawing of the platform, proposed by D. Stewart.....	5
Figure 1.5 Contemporary hexapod manipulator.....	5
Figure 1.6 Schematic drawing for the Delta robot.....	6
Figure 1.7 ABB Flexible Automation' IRB 340 FlexPicker.....	7
Figure 1.8 The agile eye parallel robot.....	8
Figure 1.9 Serial Manipulator.....	9
Figure 1.10 Parallel manipulator, Fanuc Robotics F200i.....	12
Figure 1.11 Hybrid manipulator.....	13
Figure 2.1 CAD Model of 3-CRU.....	36
Figure 2.2 Schematic Model of 3-CRU.....	37
Figure 3.1 Kinematic modeling of a leg.....	43
Figure 3.2 Stiffness mesh graphs in X with $k=500$ N/m.....	52
Figure 3.3 Stiffness mesh graphs in Y with $k=500$ N/m.....	53
Figure 3.4 Stiffness mesh graphs in Z with $k=500$ N/m.....	54
Figure 4.1 Workspace.....	57
Figure 5.1 Genetic algorithm flow chart.....	64
Figure 5.2 The best fitness and the best individuals of the design optimization.....	66

Chapter 1

Introduction

1.1 History of Robots

One of the first documented evidences of a sophisticated mechanism is that of the Clepsydra (or water clock), which was created by Ctesibius of Alexandria a Greek physicist and inventor, and can be considered as one of the first primitive robots ever made in the human history [1].

In the parallel kinematics community, Pollard's robot is well known as the first industrial parallel robot design. The first industrial robot to be built was not the above and cannot be credited to the same Willard Pollard. The engineer who co-designed the first industrial robot was Willard L.V. Pollard's son, Willard L.G. Pollard Jr. in 1942 (Figure 1.1) [2].

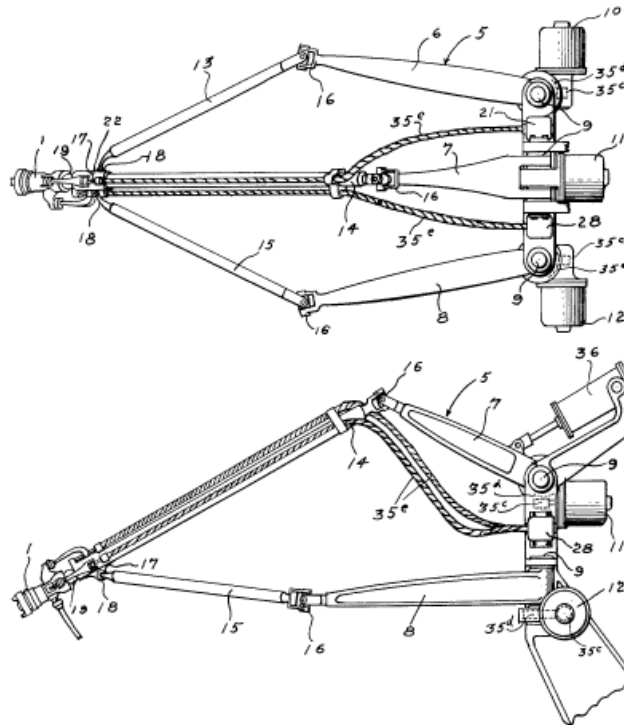


Figure 1.1 The first spatial industrial parallel robot, patented in 1942 (US Patent No. 2286571)

A couple of years later, in 1947, on the other side of the Atlantic, a new parallel mechanism was invented, the one that became the most popular, the one that changed an industry, and the one that has been replicated over a thousand times the variable length-strut octahedral hexapod (Figure 1.2) by Dr. Eric Gough [3].

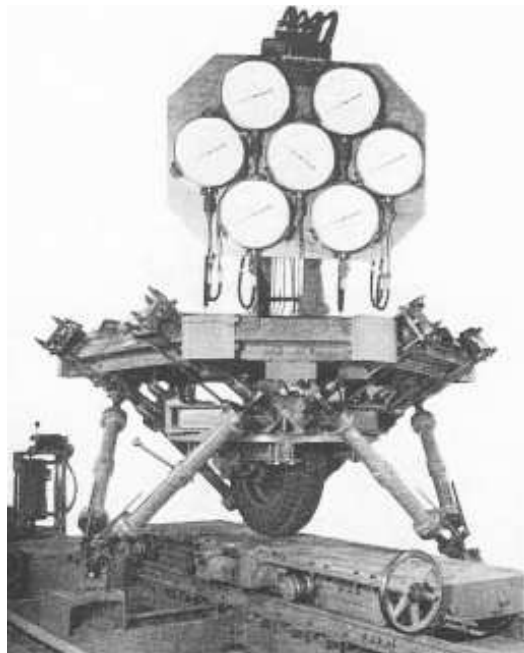


Figure 1.2 The First octahedral hexapod or the original Gough (By Dr. Eric Gough [3])

Nevertheless, during the last thirty years the robot manipulators have found their places in warehouses, laboratories, hospitals, harmful environments, even outer space. Numerous applications appeared. The majority of the industrial manipulators were and still are of the so-called serial morphology, a term that we will define precisely later. Many of the serial manipulators are of special class, called anthropomorphic.

In the late eighties, demands started appearing for robots possessing lower inertia and higher robustness, motion rapidity and precision, along with the capability of manipulating larger loads. This further pushed the research and development in terms of novel robot morphologies with improved functional characteristics. Bit by bit, the parallel robots drew bigger interest, to become a central robotic research domain with multiple

application segments: from machining operations to surgery assistance and vehicle, aircraft and spacecraft simulators. Many scientists moved in this direction, creating novel parallel robot types. Starting back from the first parallel manipulators, created during the period of 1945-1970, we could cite here some famous ones, such as:

- The Gough platform - a parallel manipulator (Figure 1.2), created in 1947 by Eric Gough. The motion simulator that Klaus Cappel developed in 1962 at the request of the Franklin Institute Research Laboratories in Philadelphia to improve an existing conventional vibration system (Figure 1.3) and the platform of D. Stewart [4] he proposed to use in a flight simulator (Figure 1.4) in 1965, can be mentioned here as well. These manipulators gave birth to the well-known class of parallel octahedral hexapods, called also hexapod positioners (Figure 1.5).

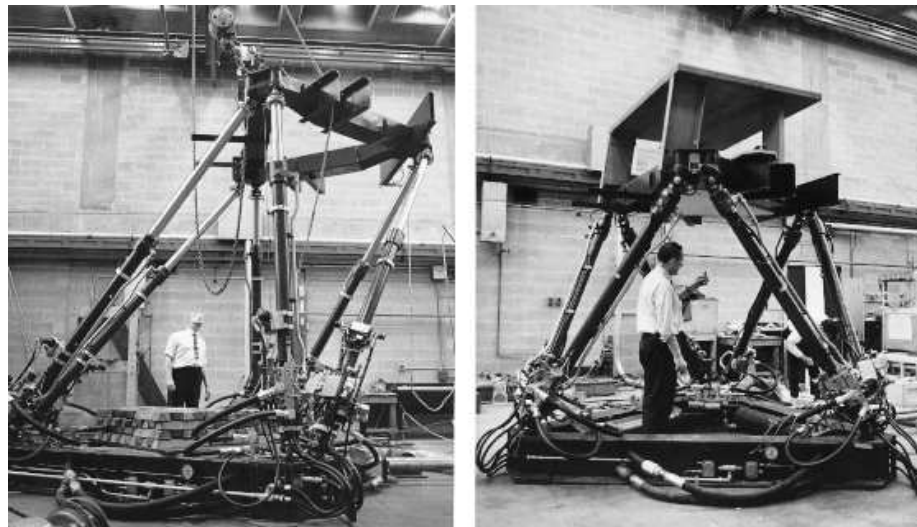


Figure 1.3 The flight simulator of Klaus Cappel, based on an octahedral hexapod
(courtesy of Klaus Cappel)

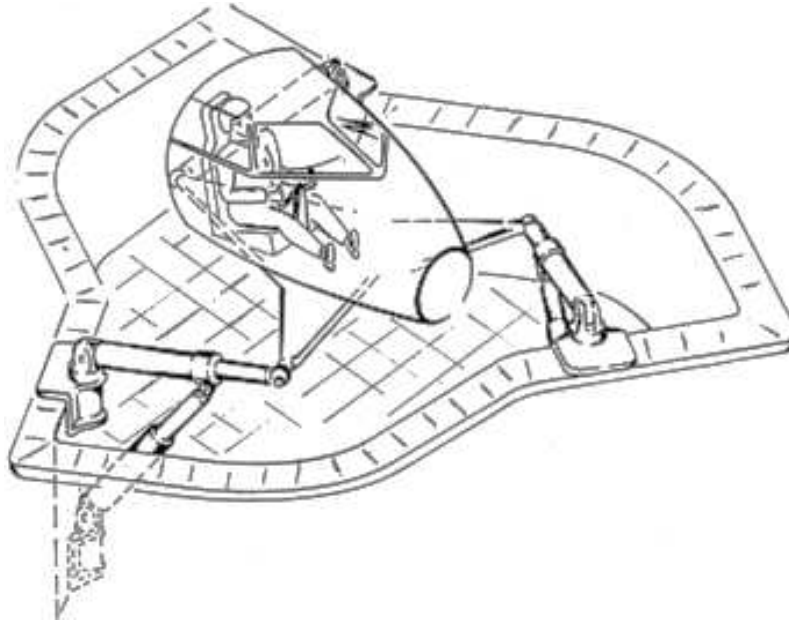


Figure 1.4 Schematic drawing of the platform (Proposed by D. Stewart [4])



Figure 1.5 Contemporary hexapod manipulator (image courtesy of PI Physik Instrumente GmbH and Co. KG.).

- The Delta robot family. The ingenious idea from the early 80s of Raymond Clavel [5], professor at the Ecole Polytechnique Federale de Lausanne, of using light parallelograms as constitutive elements of the legs of a parallel robot (Figure 1.6) gave birth to the Deltas. The use of base-mounted actuators and low-mass elements allows the manipulator to achieve accelerations of up to 50 g in experimental environments and 12 g in industrial applications, which makes it convenient for pick-and-place operations of light objects (from 10 g to 1 kg) at high speeds. Nowadays, the Delta robots find multiple applications, including industrial machining operations like drilling, etc.

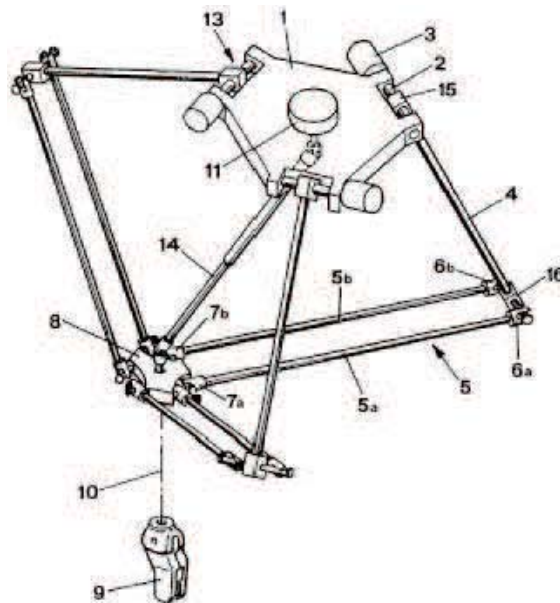


Figure 1.6 Schematic drawing of the Delta robot (from R. Clavel US patent [5]).



Figure 1.7 ABB Flexible Automation's IRB 340 FlexPicker (courtesy of ABB Flexible Automation)

- The Agile Eye (a spherical parallel mechanism) developed by Gosselin and Hamel [7] in the Robotics Laboratory at Laval University, Canada (Figure 1.8), and principally destined to fast video camera orientation tasks. Because of its low inertia and inherent stiffness, the mechanism can achieve angular velocities superior to 1000 deg/sec and angular accelerations greater than 20000 deg/sec², largely outperforming the human eye. Since it was patented in 1993, the Agile Eye has gained popularity, giving birth to some simpler, yet very effective mechanisms.

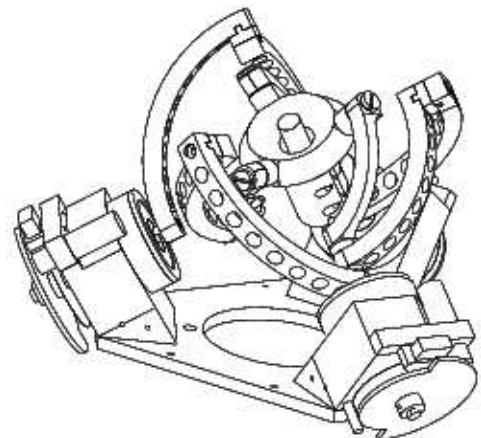
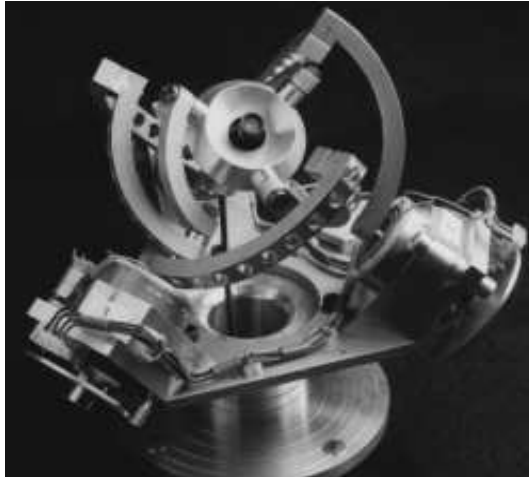


Figure 1.8 The Agile Eye parallel robot (images courtesy of Robotics Laboratory at University of Laval, Canada)

These are, of course, only some examples of widely known parallel manipulator inventions.

1.2 Robotic Architectures

This section presents the three basic architectures for robot manipulators. These architectures are characterized by the type of kinematic chains connecting the output link of the manipulator to the base link. The three basic robot architectures are:

- 1) Serial architecture
- 2) Parallel architecture
- 3) Hybrid architecture

1.2.1 Serial Architecture

This is the classical anthropomorphic architecture for robot manipulators (Figure 1.9). In this architecture, the output link is connected to the base link by a single open loop kinematic chain. The kinematic chain is composed of a group of rigid links with pairs of adjacent links that are interconnected by an active kinematic pair (controlled joint).



Figure 1.9 Serial Manipulator (taken by Jo Teichmann, Augsburg, Germany for KUKA Robot GmbH, Year 2002)

Serial manipulators feature a large work volume and high dexterity, but suffer from several inherent disadvantages. These disadvantages include low precision, poor force exertion capability and low payload-to-weight ratio, motors that are not located at the base, and a large number of moving parts leading to high inertia.

The low precision of these robots stems from cumulative joint errors and deflections in the links. The low payload-to-weight ratio stems from the fact that every

actuator supports the weight of the successor links. The high inertia is due to the large number of moving parts that are connected in series, thus forming long beams with high inertia.

Another disadvantage of serial manipulators is the existence of multiple solutions to the inverse kinematics problem. The inverse kinematics problem is defined as finding the required values of the actuated joints that correspond to a desired position and orientation of the output link. The solution of the inverse kinematic problem is a basic control algorithm in robotics; therefore, the existence of multiple solutions to the inverse kinematics problem complicates the control algorithm. The direct kinematics problem of serial manipulators has simple and single-valued solution. However, this solution is not required for control purposes. The direct kinematics problem is defined as calculating the position and orientation of the output link for a given set of actuated joints values.

The low precision and payload-to-weight ratio lead to expensive serial robots utilizing extremely accurate gears and powerful motors. The high inertia disadvantage prevents the use of serial robots from applications requiring high accelerations and agility, such as flight simulation and very fast pick and place tasks.

1.2.2 Parallel Architecture

This non-anthropomorphic architecture for robot manipulators, although known for a century, was developed mainly during the last three decades. This architecture is composed of an output platform connected to a base link by several kinematic chains (Figure 1.10). Motion of the output platform is achieved by simultaneous actuation of the

kinematic chains extremities. Similarly, the various kinematic chains support the load carried by the output link; therefore, this architecture is referred to as parallel architecture. In contrast to the open chain serial manipulator, the parallel architecture is composed of closed kinematic chains only and every kinematic chain includes both active and passive kinematic pairs.

Parallel manipulators exhibit several advantages and disadvantages. The disadvantages of the parallel manipulators are limited work volume, low dexterity, complicated direct kinematics solution, and singularities that occur both inside and on the envelope of the work volume. However, the parallel architecture provides high rigidity and high payload-to-weight ratio, high accuracy, low inertia of moving parts, high agility, and simple solution for the inverse kinematics problem. The fact that the load is shared by several kinematic chains results in high payload-to-weight ratio and rigidity. The high accuracy stems from sharing, not accumulating, joint errors.

Based on the advantages and disadvantages of parallel robots, it can be concluded that the best suitable implementations for such robots include those that require limited workspace, high accuracy, high agility, and robots that are lightweight and compact. These ideal implementations exploit both the disadvantages and advantages of the parallel architecture.

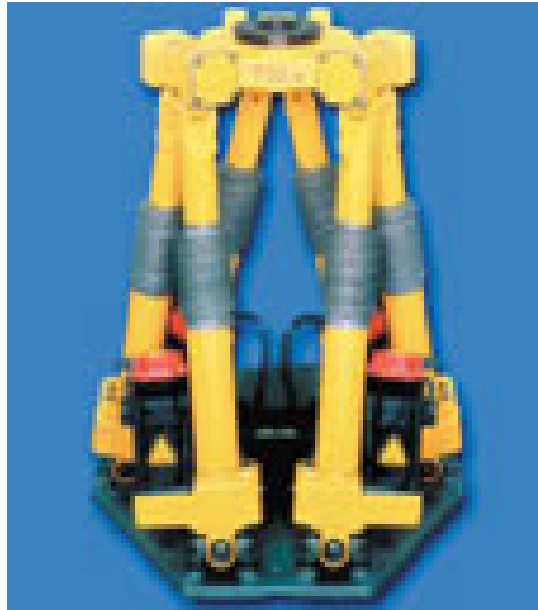


Figure 1.10 Parallel manipulator, Fanuc Robotics' F200i (courtesy of Fanuc Robotics)

1.2.3 Hybrid Architecture

The combination of both open and closed kinematic chains in a mechanism leads to a third architecture, which is referred to as the hybrid architecture. This architecture combines both advantages and disadvantages of the serial and parallel mechanisms. Figure 1.11 presents an example of a hybrid manipulator constructed from two parallel manipulators connected in series.

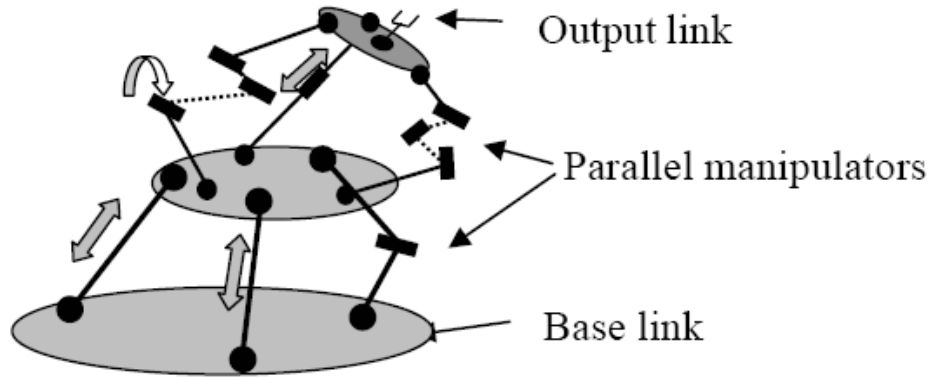


Figure 1.11 Hybrid manipulator

1.3 Fully Parallel and Non-fully Parallel Manipulators

There are two major categories of parallel robots. They are the fully parallel robots, and the non-fully parallel robots. The distinction between these categories is based on the following definition. This definition is the same as the one presented in [8].

Definition: Fully parallel manipulator

A fully parallel manipulator is a parallel mechanism satisfying the following conditions:

- 1) The number of elementary kinematic chains equals the relative mobility (connectivity) between the base and the moving platform.
- 2) Every kinematic chain possesses only one actuated joint.
- 3) All the links in the kinematic chains are binary links; i.e., no segment of an elementary kinematic chain can be linked to more than two bodies.

Based on the solution multiplicity of the inverse kinematics problem, this limiting definition can be summarized as follows. A fully parallel manipulator has one and only one solution to the inverse kinematics problem. Any parallel manipulator with multiple solutions for the inverse kinematics problem is a non-fully parallel manipulator. Table 1.1 specifies the physical characteristics of serial and parallel manipulators.

Table 1.1 Comparison between Serial and Parallel manipulators

Property	Serial Manipulator	Parallel Manipulator
Type of kinematic chains	Open kinematic chain	Closed kinematic chain
Type of joints used	Actuated joints	Actuated and passive joints
The role of actuated joints	Twist applicators	Wrench applicators
Direct kinematics problem	Simple and single-valued solution	Complicated with up to 40 solutions
Inverse kinematics problem	Complicated with multiple solutions	Simple with multiple solutions
Joint errors	Cumulative	Non-cumulative
Positional accuracy	Poor	Average
Payload-to weight ratio	Low	Very high
Singularity	Loss of freedoms	Gain and loss of freedoms
Singularity domain	On the envelope of the workspace	Both inside and on the envelope of freedoms
Jacobian mapping	Maps joint speeds to end effector linear/angular	Maps the end effector linear/angular velocity to

	velocity	actuated joint's speeds
Work volume	Large	Small
Inertia of moving parts	High	Low

1.4 Summary of the Developed Robot

The first implementation of a parallel architecture by Gough and Whitehall [3] presented six degrees of freedom tire test machine with base and moving platforms interconnected by six extensible screw jacks (Figure 1.2).

In 1965, Stewart's famous paper appeared in the proceedings of the (British) IMechE. In that paper, Mr. Stewart describes a 6 –DOF motion platform for use as a flight simulator (Figure 1.4) [4].

Later, all platforms based manipulators were called Stewart-Gough platform or Stewart platforms.

Since 1980, there has been an increasing interest in the development of parallel manipulators. Potential applications of parallel manipulators include mining machines by Cleary and Arai [9], pointing devices by Gosselin and Angeles [10], and walking machines by Waldron, Vohnout, Pery, and McGhee [11].

Hunt [12] suggested the use of parallel-actuated mechanisms like the flight simulator of Stewart as robot manipulators and mentioned that such parallel manipulators deserve detailed study in the context of robotic applications in view of their specific advantages (e.g. better stiffness and precise positioning capability) over conventional

serial robots. This can be marked as the starting point of research on parallel manipulators in general and the Stewart platform in particular in robotic applications.

The recent trend toward high-speed machining has motivated research and development of new and novel types of machine tools called parallel kinematic machines (PKMs). PKMs are based on the kinematic architecture of parallel manipulators. A parallel manipulator typically consists of a moving platform that is connected to a fixed base by several legs. The number of legs is usually at least equal to the number of degrees of freedom of the moving platform, such that each leg is driven by no more than one actuator and all actuators can be mounted on or near the fixed base. Note, that if the number of legs is less than the number of degrees of freedom, then more than one actuator will be needed in some legs. Examples of PKMs include the Variax Machining Center developed by Giddings and Lewis [13], the Octahedral Hexapod by Ingersoll [14].

Most 6-DOF PKMs are based on the Stewart-Gough platform architecture. However, six degrees of freedom are often not required for machine tools and other applications due to a high cost. Therefore, parallel manipulators with less than six degrees of freedom have attracted the researchers and some of them were used in the structure designs of robotic manipulators. For example, the 3-RPS parallel platform was adopted as a micromanipulator by Lee and Shah [16]; the 3-DOF spherical parallel platform was used in the structure design of the “agile eye” by Gosselin and Hamel [7]. The direct drive DELTA manipulator with three translational degrees of freedom was presented by Clavel [17] to meet the demand of high efficiency manipulation. Wang and Gosselin [18,19] presented a 4-DOF and a 5-DOF parallel platforms and pointed out that

they can substitute the general 6-DOF parallel platform in the cases where less than six degrees of freedom are sufficient for task manipulations.

Tsai [20] presented a 3-DOF parallel manipulator with more than three legs. The additional legs permit a separation of the function of constraint from that of actuation at a cost of increased mechanical complexity and chances of leg interference.

In a flexible automation approach to batch or job-shop production, the re-configurability of the elements of a manufacturing system has proved to be important. A key element of reconfigurable manufacturing systems is the reconfigurable machine tools (RMT). Zhang and Bi [21] introduced the theoretical design of re-configurable machine tools using modular design approach.

However, these manipulators have coupled motion between the position and orientation of the end-effector. Therefore, the kinematics model is complex and the manipulator is difficult to control.

Recent research on 3-DOF parallel manipulators has been leaning toward the decoupling of the position and orientation of the end-effector. Kinematics decoupling for a parallel manipulator is that one motion of the up-platform only corresponds to input of one leg or one group of legs. In addition, the input cannot produce other motion. Tsai et al. [22] designed a 3-DOF translational parallel manipulator that employs only revolute joints and a spatial 3-UPU (Universal-Prismatic-Universal) parallel manipulator [23]. Kim and Tsai [24] discussed the optimal design about a 3-PRRR (Prismatic-Revolute-Revolute-Revolute) manipulator. Zhao and Huang [25] studied the kinematics of an over-constrained 3-RRC (Revolute-Revolute-Cylindrical) translational manipulator, and Kong

and Gosselin [26] studied the kinematics and singularity of a 3-CRR (Cylindrical-Revolute-Revolute) translational parallel manipulator.

Chapter 2

Conceptual Design

2.1 Introduction

2.1.1 Classification of Kinematic Decoupling

The parallel manipulator whose motions are decoupled, i.e., some actuator movements influence only some motion outputs, is called a decoupled manipulator.

The classification of kinematic decoupling can be sorted as following:

Let U , the kinematic output matrix of a parallel manipulator, to be

$$U = \begin{bmatrix} x(\theta_i) & y(\theta_i) & z(\theta_i) \\ \alpha(\theta_i) & \beta(\theta_i) & \gamma(\theta_i) \end{bmatrix}, \quad i = 1 \sim M, \quad (2.1)$$

where $x(\theta_i)$, $y(\theta_i)$, and $z(\theta_i)$ denote the components of the origin coordinate of the moving coordinate system attached to the moving platform with respect to the reference coordinate system attached to the base platform, $\alpha(\theta_i)$, $\beta(\theta_i)$, and $\gamma(\theta_i)$ denote the three Euler angles of the moving coordinate system, θ_i denotes the generalized variable of the i^{th} actuator, and M denotes the mobility of the platform.

Take a 6-DOF parallel manipulator as an example; the kinematic relationship between output and input variables can be classified as follows:

- (1) If each of the independent output variable is a function of all input variables

$$\theta_i, (i = 1 \sim M),$$

such as:

$$\begin{aligned} x &= x(\theta_1, \theta_2, \dots, \theta_6) \\ y &= y(\theta_1, \theta_2, \dots, \theta_6) \\ z &= z(\theta_1, \theta_2, \dots, \theta_6) \\ \alpha &= \alpha(\theta_1, \theta_2, \dots, \theta_6) \\ \beta &= \beta(\theta_1, \theta_2, \dots, \theta_6) \\ \gamma &= \gamma(\theta_1, \theta_2, \dots, \theta_6) \end{aligned} \tag{2.2}$$

the relationship between input and output variables is called coupling.

- (2) If each of the independent output variable corresponds to only one input variable,

such as:

$$\begin{aligned} x &= x(\theta_1) \\ y &= y(\theta_2) \\ z &= z(\theta_3) \\ \alpha &= \alpha(\theta_4) \\ \beta &= \beta(\theta_5) \\ \gamma &= \gamma(\theta_6) \end{aligned} \tag{2.3}$$

the relationship between input and output variables is called complete decoupling .

- (3) If the situation that is consistent with neither case (1) nor case (2) is called partial decoupling. For instance:

$$\begin{aligned}
x &= x(\theta_1, \theta_2, \theta_3, \theta_4, \theta_5, \theta_6) \\
y &= y(\theta_1, \theta_2, \theta_3, \theta_4, \theta_5) \\
z &= z(\theta_1, \theta_2, \theta_3, \theta_4) \\
\alpha &= \alpha(\theta_1, \theta_2, \theta_3) \\
\beta &= \beta(\theta_1, \theta_2) \\
\gamma &= \gamma(\theta_1)
\end{aligned} \tag{2.4}$$

Although the complete decoupling is a perfect model for the task specified, designing mechanisms to truly realize this model is very difficult. Nevertheless, realizing partial decoupling is also of significance especially when most of the known parallel manipulators belong to the type of strong coupling. The high decoupling of a mechanism makes kinematics and dynamics analyses easy, which can evidently simplify the control and path planning of the manipulator. Therefore, from the point of view of improving work performance of manipulators, it is necessary to investigate and synthesize decoupled parallel manipulators.

2.1.2 Isotropy

We know that the Jacobian matrix of robotic manipulator is the matrix mapping (i) the actuated joint velocity space, and the end-effector velocity space, and (ii) the static load on the end-effector and the actuated joint forces or torques. Isotropic of a robotic manipulator is related to the condition number of its Jacobian matrix, which can be calculated as the ratio of the largest and the smallest singular values. A robotic manipulator is fully isotropic if its Jacobian matrix is isotropic throughout the entire workspace, i.e., the condition number of the Jacobian matrix is equal to one. Thus, the

condition number of the Jacobian matrix is an interesting performance index characterizing the distortion of a unit ball under this linear mapping. The condition number of the Jacobian matrix was first used by Salisbury and Craig [34] to design mechanical fingers, and then developed by Angeles [35] as a kinematic performance index of robotic mechanical systems. The isotropic design improves kinematic and dynamic performance [36].

For parallel manipulators, the velocities of the moving platform are related to the velocities of the actuated joint $[\dot{\phi}]$ by general equation:

$$[\mathbf{A}] \begin{bmatrix} v \\ \omega_p \end{bmatrix} = [\mathbf{B}] \begin{bmatrix} \dot{q} \end{bmatrix} \quad (2.5)$$

where $[v] = [v_x v_y v_z]^T$ is the velocity of a point P belonging to the moving platform, $[\omega] = [\omega_x \omega_y \omega_z]^T$ is the angular velocity of the moving platform, $[\mathbf{A}]$ is the direct Jacobian, $[\mathbf{B}]$ is the inverse Jacobian, and O is the coordinate system in which the velocities of the moving platform are expressed.

Equation (2.5) can also be written as a linear mapping between joint velocities and the velocities of the moving platform.

$$\begin{bmatrix} v \\ \omega_p \end{bmatrix} = [\mathbf{J}] [\dot{\phi}] \quad (2.6)$$

$$\text{where } [\mathbf{J}] = [\mathbf{A}]^{-1}[\mathbf{B}] \quad (2.7)$$

is the global Jacobian including the direct and inverse Jacobians. For many architectures of parallel manipulators, it is more convenient to study the conditioning of the Jacobian that is related to the inverse transformation, i.e., $[\mathbf{J}]^{-1} = [\mathbf{B}]^{-1}[\mathbf{A}]$

The isotropic conditions should apply to either Jacobian matrices \mathbf{A} and \mathbf{B} or only to Jacobian matrix \mathbf{J} or (\mathbf{J}^{-1}) . If we have a matrix \mathbf{Q} (which can be \mathbf{A} , \mathbf{B} , \mathbf{J} , or \mathbf{J}^{-1}) whose all entries have the same units, then we can define its condition number $k(\mathbf{Q})$ as a ratio of the largest singular value τ_1 of \mathbf{Q} and the smallest one τ_2 . We note that $k(\mathbf{Q})$ can attain values from 1 to infinity. The condition number attains its minimum value of unity for matrices with identical singular values.

We know that the singular values of \mathbf{Q} are given by the square roots of the eigenvalues of $[\mathbf{Q}]^T[\mathbf{Q}]$. A matrix \mathbf{Q} is isotropic if $[\mathbf{Q}]^T[\mathbf{Q}]$ is proportional to an identity matrix \mathbf{I} . So, the Jacobian matrices \mathbf{A} , \mathbf{B} , \mathbf{J} , or \mathbf{J}^{-1} are isotropic if [15]

$$[\mathbf{A}]^T[\mathbf{A}] = \sigma_1^2 [\mathbf{I}] \quad (2.8)$$

$$[\mathbf{B}]^T[\mathbf{B}] = \sigma_2^2 [\mathbf{I}] \quad (2.9)$$

$$[\mathbf{J}]^T[\mathbf{J}] = \sigma_3^2 [\mathbf{I}] \quad (2.10)$$

$$[\mathbf{J}]^{-1}[\mathbf{J}]^T = \sigma_4^2 [\mathbf{I}] \quad (2.11)$$

where σ_i ($i = 1,2,3,4$) is a scalar.

2.1.3 Screw Theory and Mobility Analysis

2.1.3.1 Screw and Reciprocal Screws

Screw theory was developed by Sir Robert Stawell Ball in 1876 [32], for application in kinematics and statics of mechanisms (rigid body mechanics). It is a way to express displacements, velocities, forces, and torques in three-dimensional space, combining both rotational and translation parts. Recently, screw theory has regained importance and has become an important tool in robot mechanics, mechanical design, computational geometry, and multi-body dynamics.

In screw theory [33], a straight line in space can be expressed by two vectors, \mathbf{S} and \mathbf{S}_0 . Their dual combination is called a line vector

$$\mathcal{S} = (\mathbf{S}; \mathbf{S}_0) = (\mathbf{S}; \mathbf{r} \times \mathbf{S}) = (l \ m \ n; o \ p \ q) \quad (2.12)$$

where \mathbf{S} is the unit vector along a straight line or a screw axis; l , m , and n are the three direction cosines of \mathbf{S} ; o , p , and q are the three elements of the cross product of \mathbf{r} and \mathbf{S} ; \mathbf{r} is a position vector of any point on the line or screw axis. The $(\mathbf{S}, \mathbf{S}_0)$ is also called the Plucker coordinates for the line vector and it consists of six components in total.

For a line vector, $\mathbf{S} \cdot \mathbf{S}_0 = 0$. When $\mathbf{S} \cdot \mathbf{S}_0 = 1$, it is a unit line vector. When $\mathbf{S} \cdot \mathbf{S}_0 \neq 0$, it is a screw $\mathcal{S} = (\mathbf{S}; \mathbf{S}_0) = (\mathbf{S}; \mathbf{r} \times \mathbf{S} + h\mathbf{S})$ and its pitch is finite. If the pitch of a screw is equal to zero, the screw degenerates to a line vector. In other words, a unit screw with zero-pitch ($h = 0$) is a line vector. The line vector can be used to express a revolute pair in

kinematics, or a unit force in static along the line in space. If the pitch of a screw goes to infinity, $h = \infty$, the screw is defined as

$$\mathcal{S} = (0; \mathbf{S}) = (0 \ 0 \ 0; l \ m \ n) \quad (2.13)$$

and called a couple in screw theory, which means a unit screw with infinity-pitch ($h = \infty$) is a couple. The couple can be used to express a prismatic pair in kinematics or a couple in statics. \mathbf{S} is its direction cosine.

Both the revolute joint and prismatic joint is of the single-DOF kinematic pair. The multi-DOF kinematic pairs, such as cylinder joint, universal joint, or spherical joint can also be represented by a group of screws because of its kinematic equivalency to a combination of revolute and prismatic pairs.

The reciprocal product of two screws, say $\mathcal{S} = (\mathbf{S}; \mathbf{S}_0)$ and, $\mathcal{S}^r = (\mathbf{S}^r; \mathbf{S}_0^r)$ is defined as [33] [61]

$$\mathcal{S} \circ \mathcal{S}^r = \mathbf{S} \cdot \mathbf{S}_0^r + \mathbf{S}^r \cdot \mathbf{S}_0 \quad (2.14)$$

Where, the symbol “o” denotes the reciprocal product of two screws. The reciprocal product of two screws represents the work produced by a wrench acting on a rigid body undergoing an infinitesimal twist.

Two screws are said to be reciprocal if their reciprocal product is zero

$$\mathcal{S} \circ \mathcal{S}^r = lo^r + mp^r + nq^r + ol^r + pm^r + qn^r = 0 \quad (2.15)$$

Equation (2.15) shows that the wrench \mathcal{S}^r acting on a rigid body undergoing an infinitesimal twist \mathcal{S} yields no work. Then, the wrench \mathcal{S}^r denotes a constraint force when its pitch is zero, or a constraint couple when its pitch is infinite. The former restricts a translational freedom of the rigid body along the direction of the force, and the latter restricts a rotational freedom around the axis of the couple.

The reciprocal equation of two screws is also expressed as follows [61]:

$$(h_1 + h_2) \cos \lambda_{12} - r_{12} \sin \lambda_{12} = 0 \quad (2.16)$$

Where, r_{12} is the normal distance of the two screws and λ_{12} is the twist angle between the two screws. Clearly, when two line vectors intersect or are parallel to each other, the two screws are reciprocal.

According to equations (2.15) and (2.16), some useful reciprocal conditions for two screws can be concluded simply as in Table 2.1.

Table 2.1 Reciprocal conditions for two screws

Number	Reciprocal conditions
1	The sufficient and necessary condition for reciprocity of two line vectors is coplanar.
2	Any two couples are consequentially reciprocal
3	A line vector and a couple are reciprocal only when they are perpendicular
4	Any two screws are consequentially reciprocal when they are perpendicular and intersecting
5	Both the line vector and couple are self-reciprocal, respectively

For mobility analysis, from equation (2.15) we can get the reciprocal screws. Sometimes, using Table 2.1 is more convenient than that of equation (2.15). The correctness of these two methods is often proven by each other.

Furthermore, reciprocity of screws is origin independent, which is easy to prove from equation (2.16). There also exist similar results for the linear dependency of screws.

2.1.3.2 Screw Systems and Reciprocal Screw Systems

A screw system of order N ($0 \leq N \leq 6$) comprises all the screws that are linearly dependent on N given linearly independent screws. A screw system of order N is also called an N -system. Any set of N linearly independent screws within an N -system forms a basis of the N -system. Usually, the basis of an N -system can be chosen in different ways. Given an N -system, there is a unique reciprocal screw system of order $(6 - N)$, which comprises all the screws reciprocal to the original screw system.

2.1.3.2 Twist Systems and Wrench Systems

A screw $\$$ multiplied by a scalar ρ , i.e., $\rho \$$, is called a twist if it represents an instantaneous motion of a rigid body, and a wrench if it represents a system of forces and couples acting on a rigid body.

The twist system of a kinematic chain, in the form of a kinematic joint, serial kinematic chain or parallel kinematic chain, is an f -system where $f \leq F$ and F denotes the DOF of the kinematic chain. The wrench system of a kinematic chain is a $(6 - f)$ -system. The twist system of a kinematic chain is the reciprocal screw system of its wrench system, and vice versa.

The twist systems and wrench systems of revolute (R) joint, prismatic (P) joint, universal (U) joint and Cylinder (C) joint are presented below.

- (i) R (Revolute) joint

The twist system of an R joint is a 1-system. The wrench system is a 5-system

(ii) P (Prismatic) joint

The twist system of a P joint is a 1-system. The wrench system is a 5-system

(iii) U (universal) joint

The twist system of a U joint is a 2-system. The wrench system is a 4-system

(iv) C (Cylinder) joint

The twist system of a C joint is a 2-system. The wrench system is a 4-system

2.1.3.3 Mobility Analysis Based on Screw Theory

The general Chebyshev-Grubler- Kutzbach formula is:

$$M = d(\eta - g - 1) + \sum_{i=1}^g f_i \quad (2.17)$$

where:

M : Mobility or the degree of freedom of the system.

d : The order of the system ($d = 3$ for planar mechanism, and $d = 6$ for spatial mechanism).

η : The number of the links including the frames.

g : The number of joints.

f_i : The number of degrees of freedom for the i th joint.

One drawback of the Chebyshev-Grubler-Kutzbach formula is that it can only derive the number of DOF of some mechanisms, but cannot obtain the properties of the DOF, i.e., whether they are translational or rotational DOF.

For a lower-mobility parallel mechanism, each leg exerts some structural constraints on the moving platform. The combined effect of all the leg structural constraints determines the mobility of the mechanism. We use the leg constraint system to describe the structural constraints of a single leg, which is defined as a screw system formed by all screws reciprocal to the unit twist associated with all kinematic pairs in a leg. We use the mechanism constraint system to describe the combined effect of all leg constraints.

Based on linear dependency of the leg structural constraints under different geometrical conditions, we can obtain the mechanism constraint system as well as the constrained DOF of the moving platform.

Because twists and wrenches are instantaneous, it is necessary to identify whether the mechanism is instantaneous. This can be obtained by verifying the mechanism constraint system after any arbitrary finite displacement. If the mechanism constraint system remains unchanged, the mechanism is non-instantaneous. Such verification can be done by simple analysis and inspection of structural or geometrical conditions among the kinematic pairs in each leg and the mechanism. It is not necessary to know the analytical expressions of the mechanism constraints including the analytical expressions of the finite displacements in all joints of each leg.

Let $\$_{ij}$ represent the unit twist associated with the j^{th} kinematic pair in the i^{th} leg; $\$_{ij}^r$ is used to represent the j^{th} unit wrench exerted by the i^{th} leg; $\$_{mj}$ is used to represent the j^{th} unit twist in the mechanism twist system; $\$_{mj}^r$ is used to represent the j^{th} unit wrench in the mechanism constraint system.

Assume that a M-DOF ($M < 6$) parallel mechanism has ξ legs and each leg exerts ζ structural constraints on the moving platform. The $\xi \cdot \zeta$ constraints form the mechanism constraint system, which must be a $6-M$ system in the general non-singular configuration.

Because most of the lower-mobility parallel mechanisms are over-constrained, it is necessary to take the common constraints of mechanism and the passive constraints into consideration in mobility analysis. Thus, we rewrite the general Chebyshev-Grubler-Kutzbach formula as

$$M = d(\eta - g - 1) + \sum_{i=1}^g f_i + \nu \quad (2.18)$$

where ν is the number of passive constraints.

The order of a mechanism is given by

$$d = 6 - \varepsilon \quad (2.19)$$

where ε is the number of the common constraints. The common constraint is defined as a screw reciprocal to all unit twists associated with kinematic pairs in a lower-mobility parallel mechanism. A common constraint exists if and only if each leg provides one constraint and all the ξ constraints are coaxial; namely, they form an 1-system.

Considering the remaining leg constraints except those leg constraints, which form the common constraints. If they are linearly dependent, there exist passive constraints.

Assume that the remaining leg constraints form a l - system, the number of passive constraints is given by

$$\nu = \xi \cdot \zeta - \varepsilon \cdot \xi - l \quad (2.20)$$

It should be noted that the $\xi \cdot \zeta$ leg constraints must equal the sum of the $6-M$ mechanism constraints, the leg constraints which form the common constraints, and the passive constraints. Considering that each common constraint constrains one DOF of the moving platform, we have

$$\xi \cdot \zeta = (6 - M - \varepsilon) + \varepsilon \cdot \xi + \nu \quad (2.21)$$

Thus, a general mobility criterion for the lower-mobility parallel mechanisms can also be obtained [62]

$$M = 6 - \xi \cdot \zeta + \varepsilon(\xi - 1) + \nu \quad (2.22)$$

Equations (2.20) and (2.22) are actually established based on constraint analysis. They're applicable to both symmetrical and asymmetrical lower-mobility parallel mechanisms.

The mobility analysis of lower-mobility parallel manipulators can be performed following the steps below:

Step 1 In the initial configuration, first write out the leg twist system, and then obtain the leg constraint system. Hence, ζ is available in this step.

Step 2 According to the linear dependency of all leg constraints under different geometrical conditions obtain the mechanism constraint system as well as the constrained freedoms. In this step, ε and ν are also available.

Step 3 Check whether the mechanism is instantaneous. Simply judging if the mechanism constraint system remains unchanged after any non-singular feasible finite displacement can do this.

Step 4 Use equations (2.19) and (2.22) to verify the mobility.

2.1.4 Over-Constrained Parallel Manipulator

Usual parallel manipulators, like the Stewart platform, suffer from the problems of difficult forward kinematics, coupled motion, and small workspace, so as to make motion planning and control difficult in applications. The parallel manipulator with lower mobility ($DOF < 6$) can relatively reduce the complexity. However, most of the parallel manipulators with lower mobility are over-constrained when assembly errors are considered [29].

Over-constrained parallel kinematic manipulators are those with limbs that provide similar constraint(s) [12]. That is, the other limb also provides the motion constraint provided by one limb. These over-constrained mechanisms do move despite the fact that Grubler / Kutzbach criterion in its original form [6,12,30] concludes that they should not, and they (over-constrained mechanisms) are mobile only when certain geometrical conditions are satisfied. Although they have some advantages, such as using fewer joints and links, resulting in a simple mechanism, the main price of these over-constrained mechanisms is the need for strict manufacturing tolerance and the excessive loads on some links and/or joints. Therefore, these parallel manipulators cannot be assembled without joint clearance, which imposes negative impacts on the accuracy of the end-effector.

However, using inactive joints can reduce the number of over-constraints of a parallel manipulator [31].

2.2 Geometrical Design

In this section, we focus on the conceptual design of a 3-DOF non-over constrained translational PKM with decoupled motions. It can be used for parts assembly and light machining tasks that require large workspace, high dexterity, high loading capacity, and considerable stiffness. Kinematically, a 3-DOF non-over constrained PKM also implies that each leg should have an inactive joint.

To simplify the design and development efforts, we have the following additional considerations:

- The PKM is composed of a base and a moving platform connected by three legs
- Symmetric design - each leg is identical to the others. Hence, each leg should have the same number of actuated joints.
- Type of joints – four types of commonly used joints are considered:
 - (i) 1-DOF revolute (R) joint
 - (ii) 1-DOF prismatic (P) joint
 - (iii) 2-DOF universal (U) joint
 - (iv) 2-DOF cylinder (C) joint

Among them, the revolute and universal joints are only meant for passive (i.e. not actuated) joint, the prismatic or the prismatic in the cylinder joints are only meant for actuated joints.

- Actuated joints are placed close to the base so as to reduce the moment of inertia and increase the loading capacity and motion acceleration.

- At most one (actuated) prismatic or cylinder joint can be employed in each of the legs due to its heavy and bulky mechanical structure.
- The number of redundant DOF of a leg is not greater than one (1).
- The number of inactive joint of all legs is not greater than one (1).
- Each leg is composed of a group of at least three revolute joints with parallel axes and at most one revolute joint whose axis is not parallel to the axes of the revolute joints in the group of revolute joints with parallel axes, while the axis of the actuated joint (prismatic or cylinder) is not perpendicular to the axes of the revolute joints in the group of revolute joints with parallel axes.
- The axes of all the revolute joints in the group of revolute joints with parallel axes are not parallel to a plane.
- The axes of all three actuated joints should be arranged perpendicular to each other to satisfy the parallel manipulator featuring decoupled motion.

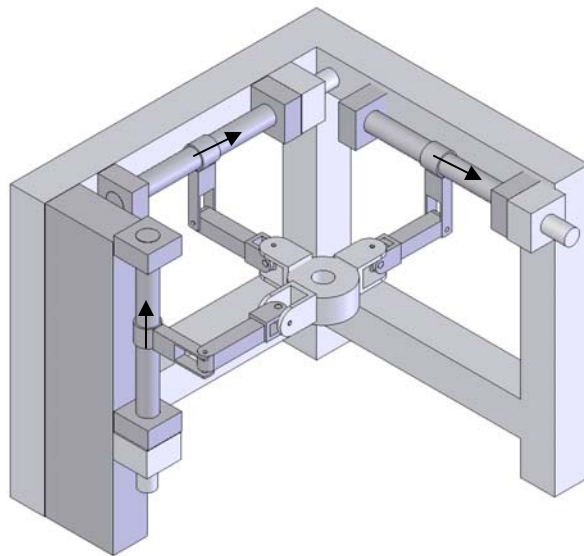
With these design considerations, a novel 3-CRU non-over constrained translational PKM with decoupled motions has been proposed. The 3-CRU (Figure 2.1) is composed of a base and a moving platform connected by three CRU legs.

The axes of the C and R joints, as well as the axe of the U joint, are arranged such that their joint axes are parallel to a common plane. As a result, the axe of outer R joint (the one connects to the moving platform) of the U joint is perpendicular to the axe of the U joint as well as all the axes of the C and R joints within a given leg. All above guarantee that instantaneous rotation of the moving platform about a direction that is perpendicular to the common plane of all the axes of the C, R, and inner R of the U joint is impossible. Since each C joint can be considered as a combination of one R joint and

one P joint with parallel axes, each U joint consists of two intersecting R joints; each leg is kinematically equivalent to a PRRRR chain.

Through preliminary analysis, a 3-DOF PKM with such three CRU legs possesses the following advantages:

- ❖ Simple kinematics and easy for analysis, design, trajectory planning, and motion control
- ❖ Large and well shaped workspace
- ❖ High stiffness
- ❖ High loading capacity



“ \rightarrow ” is the direction of the liner motor

Figure 2.1 CAD Model of 3-CRU

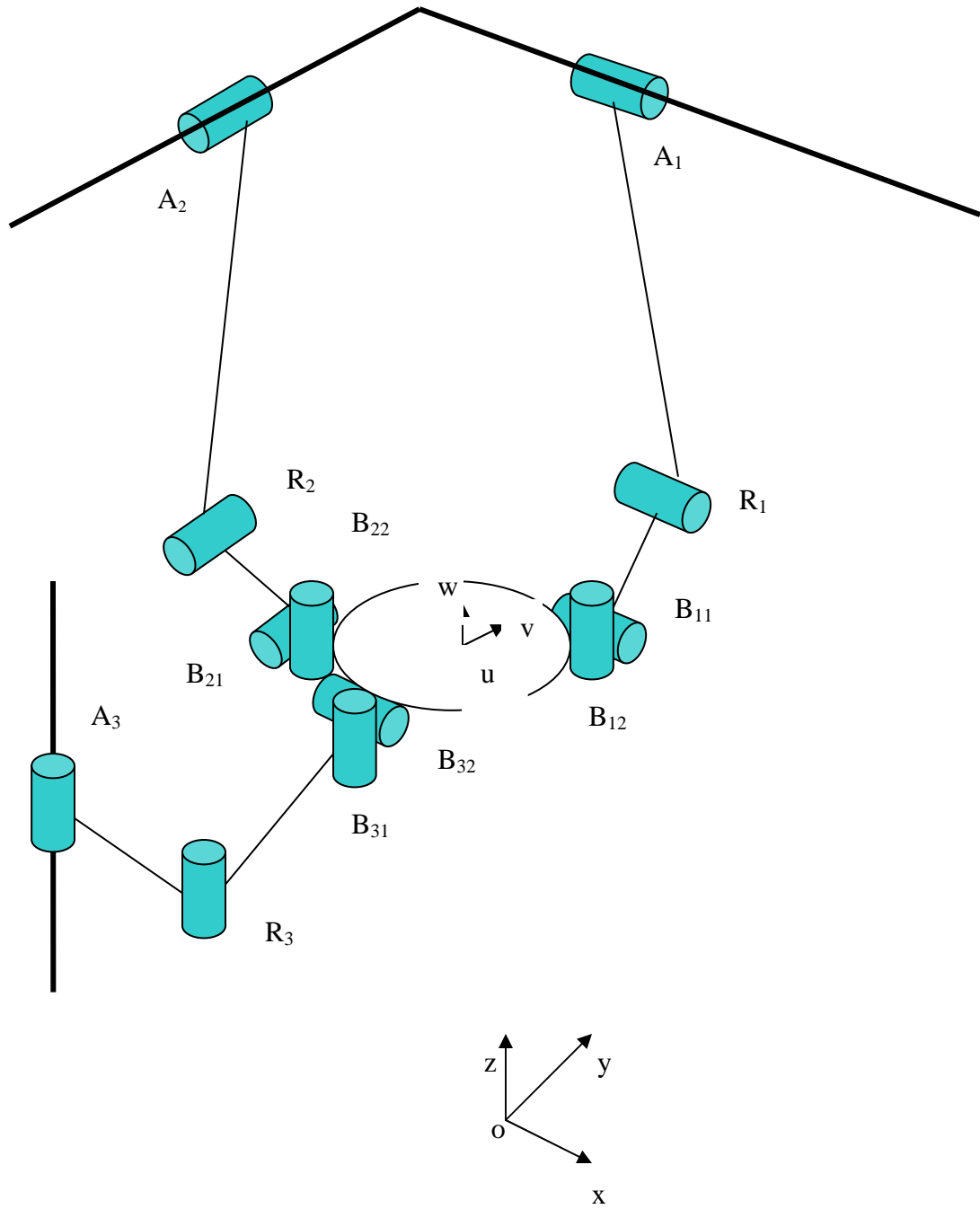


Figure 2.2 Schematic Model of 3-CRU

2.3 Mobility Analysis of the Manipulator

For the 3-CRU manipulator, we have $\zeta = 1$, and mechanism obviously contains no common constraints and redundant constraints, then we have $\varepsilon = 0$, and $\nu = 0$.

Using equation (2.18), we have:

$$M = 6 * (8 - 9 - 1) + 3 * (2 + 1 + 2) + 0 = 3 \quad (2.23)$$

Using equation (2.22), we have

$$M = 6 - 3 * 1 + 0 = 3 \quad (2.24)$$

For a parallel manipulator with less than six degrees of freedom, the motion of each leg that can be treated as a twist system is guaranteed under some exerted structural constraints, which are termed as a wrench system. The wrench system is a reciprocal screw system of the twist system for the same leg, and a wrench is said to be reciprocal to a twist if the wrench produces no work along the twist. The mobility of the manipulator is then determined by the combined effect of wrench systems of all legs.

For the 3-CRU manipulator, the wrench system of a leg is a 1-system, which exerts one constraint couple to the moving platform with its axis perpendicular to the axis of C joint within the same leg. The wrench system of the moving platform, that is a linear combination of wrench systems of all the three legs, is a 3-system, because the three wrench 1-systems consist of three couples, which are linearly dependent and form a screw 3-system. Since the arrangement of all the joints shows on Figure 2.1, the wrench systems restrict three rotations of the moving platform with respect to the fixed base at any instant, thus leading to a translational parallel manipulator.

2.4 Inactive Joint

A general leg for a translational parallel manipulator with a linear actuator is composed of $(\psi - 1)$ R joints and one P or C joints. For the purposes of simplification, the P joint (or the P joint of the C joint) is labeled with 1, while the R joints (including the R joint of C joint) are labeled with 2, 3, ..., and ψ is the sequence from the base to the moving platform.

The infinitesimal change of orientation of the moving platform is a serial kinematic chain undergoing infinitesimal joint motion is [31]

$$\Delta R = \sum_{i=2}^n (\Delta \theta_i \mathbf{s}_i) \quad (2.25)$$

where ΔR and $\Delta \theta_i$ denote the infinitesimal change of orientation of the moving platform and the infinitesimal joint motion of joint i respectively; \mathbf{s}_i denotes the unit vector along the axis of joint i before the infinitesimal motion.

For a translational parallel manipulator, there exists

$$\Delta R = 0 \quad (2.26)$$

Substitution of equation (2.25) into equation (2.26), yields

$$\sum_{i=2}^n (\Delta \theta_i \mathbf{s}_i) = 0 \quad (2.27)$$

For the 3-CRU parallel manipulator, the only R joint whose axis is not parallel to the axes of the other R joints is labeled with 5. It exists

$$\mathbf{s}_5 \neq \mathbf{s}_4 = \mathbf{s}_3 = \mathbf{s}_2 \quad (2.28)$$

Substitution of equation (2.28) into equation (2.27), yields

$$\mathbf{s}_5 \Delta\theta_5 + \sum_{i=2}^4 \Delta\theta_i \mathbf{s}_i = 0 \quad (2.29)$$

To satisfy equation (2.29), we have

$$\Delta\theta_5 = 0 \quad (2.30)$$

and

$$\sum_{i=2}^4 \Delta\theta_i = 0 \quad (2.31)$$

Equation (2.30) proves that the outer R joint of the U joint of each leg is inactive.

Equation (2.31) shows that the R joints with parallel axes within the same leg constitute a dependent joint group.

An inactive joint is a joint in a leg whose joint variable is constant during the motion of the manipulator. Although when an inactive joint is removed, the relative motion within the leg will not be changed, by using inactive joints, the number of over-constraints of the translational parallel manipulator in this thesis can be reduced.

Chapter 3

Kinematic Modeling of the 3-CRU Parallel

Manipulator

3.1 Introduction

The kinematics of a robot deal with finding the analytical relations between its input variables (the values of the actuated joints) and output variables (the position and orientation of the moving platform); the equations that connect the input and the output variables of a mechanism are called the kinematic equations of the mechanism. The equations that connect input and output velocities in a mechanism are called the instantaneous kinematic variables of the robot, i.e., the position and orientation of the moving platform, for a given set of input variables, namely, the actuated joints' variables. The inverse kinematics problem deals with finding the required input variables (actuated joints' values) that correspond to a given set of output variables (position and orientation of the moving platform).

The inverse kinematics problem of the Stewart-Gough manipulator [6] is trivial with single solution, but when the number of kinematic chains is reduced, the number of solutions of the inverse kinematics problem increases and the problem becomes more challenging. The direct kinematics problem of parallel manipulators is by far more challenging than the inverse kinematics problem since it requires solving a set of polynomial equations in the output variables. While the inverse kinematics problem for a general Stewart-Gough manipulator has only one solution, the direct kinematic problem has up to forty (40) real solutions [30]. Dietmaier [65] systematically changed the geometric properties of a general Stewart-Gough manipulator and for the first time, gave an example of a manipulator with forty (40) real solutions to the direct kinematics problem.

3.2 Inverse Kinematics

The purpose of the inverse kinematics issue is to solve the actuated variables from a given position of the mobile platform.

To facilitate the analysis, referring to Figure 3.1, we define a fixed reference frame $O-xyz$ at the centered point O on the base and a moving reference frame $P-uvw$ at the centered point P on the moving platform, with the z and w axes perpendicular to the platform, and the x and y axes parallel to the u and v axes, respectively. The direction of the i th fixed C joint is denoted by unit vector \mathbf{c}_i . A reference point M_i is defined on the axis of the i th fixed C joint, and the sliding distance is defined by d_i ;

Since the moving platform of a 3-CRU possesses only translational motion, ${}^o\mathbf{R}_p$ becomes an identity matrix. Then, we have

$$\mathbf{b}_i = {}^p\mathbf{b}_i \quad (3.1)$$

Referring to Figure 3, a vector-loop equation can be written for each leg as follows:

$$\mathbf{u}_i = \mathbf{p} + \mathbf{b}_i - \mathbf{m}_i - d_i\mathbf{c}_i \quad (3.2)$$

Substituting equation (3.1) into equation (3.2), we have:

$$\mathbf{u}_i = \mathbf{p} + {}^p\mathbf{b}_i - \mathbf{m}_i - d_i\mathbf{c}_i \quad (3.3)$$

As vectors \mathbf{u}_i and \mathbf{r}_i are orthogonal, we yield:

$$\mathbf{u}_i^T \mathbf{r}_i = 0 \quad (3.4)$$

Substituting equation (3.3) into equation (3.4), we get:

$$(\mathbf{p} + {}^p\mathbf{b}_i - \mathbf{m}_i - d_i\mathbf{c}_i)^T \mathbf{r}_i = 0 \quad (3.5)$$

For geometric parameters of this parallel manipulator, we have:

$$\mathbf{c}_1 = \mathbf{r}_1 = [1,0,0]^T \quad (3.6)$$

$$\mathbf{c}_2 = \mathbf{r}_2 = [0,1,0]^T \quad (3.7)$$

$$\mathbf{c}_3 = \mathbf{r}_3 = [0,0,1]^T \quad (3.8)$$

$$\mathbf{e}_1 = [0,0,1]^T \quad (3.9)$$

$$\mathbf{e}_2 = [0,0,1]^T \quad (3.10)$$

$$\mathbf{e}_3 = [1,0,0]^T \quad (3.11)$$

Substituting equations (3.6) to (3.11) into equation (3.5), we yield the solution of the inverse displacement analysis for the 3-CRU parallel manipulator as:

$$d_1 = p_x + b_{x1} - m_{x1} \quad (3.12)$$

$$d_2 = p_y + b_{y2} - m_{y2} \quad (3.13)$$

$$d_3 = p_z + b_{z3} - m_{z3} \quad (3.14)$$

From equations (3.12) to (3.14), we can easily observe that the motions of the 3-CRU parallel manipulator are decoupled. The actuator in leg 1 controls the translation along the X direction; the actuator in leg 2 controls the translation along the Y direction while the actuator in leg 3 controls the translation along Z direction.

The distance between the center of the moving plate and base is $m_i = l_{2i} + b$

3.3 Forward Kinematics

The forward kinematics is to obtain the end-effector position, $[p_x, p_y, p_z]^T$, when the input sliding distance d_i is given.

By solving Equations (3.12) to (3.14) for variables x , y , and z , the forward kinematics can be performed. Thus, we yield:

$$p_x = d_1 - b_{x1} + m_{x1} \quad (3.15)$$

$$p_y = d_2 - b_{y2} + m_{y2} \quad (3.16)$$

$$p_z = d_3 - b_{z3} + m_{z3} \quad (3.17)$$

3.4 Velocity Analysis

Equations (3.15) to (3.17) can be rewritten as:

$$\begin{bmatrix} d_1 \\ d_2 \\ d_3 \end{bmatrix} = \begin{bmatrix} p_x + b_{x1} - m_{x1} \\ p_y + b_{y2} - m_{y2} \\ p_z + b_{z3} - m_{z3} \end{bmatrix} \quad (3.18)$$

Taking the derivative of equation (3.18) with respect to time yields:

$$\begin{bmatrix} \dot{d}_1 \\ \dot{d}_2 \\ \dot{d}_3 \end{bmatrix} = \mathbf{J} \begin{bmatrix} \dot{p}_x \\ \dot{p}_y \\ \dot{p}_z \end{bmatrix} \quad (3.19)$$

where \mathbf{J} is the 3 x 3 identity matrix. Since \mathbf{J} is an identity matrix, the manipulator is isotropic everywhere within its workspace.

Therefore, the velocity equations of the 3-CRU parallel manipulator can be written as:

$$\begin{aligned} \dot{d}_1 &= \dot{p}_x \\ \dot{d}_2 &= \dot{p}_y \\ \dot{d}_3 &= \dot{p}_z \end{aligned} \quad (3.20)$$

3.5 Singularity Analysis

3.5.1 Constraint Singularity

The constraint singularity [63] occurs when the moving platform of a translational parallel manipulator can rotate instantaneously. The constraint singularity occurs for a

translational parallel manipulator if and only if its wrench system (a 3-system of ∞ – pitch) degenerates into a 2-system or a 1-system.

For the 3-CRU translational parallel manipulator, as $\mathbf{r}_i \neq \mathbf{e}_i$, the CRU leg exerts one constraint on the moving platform, which prevents it from rotating about any axis parallel to $\mathbf{r}_i \times \mathbf{e}_i$. Therefore, the wrench system of the leg is invariant. The order of the wrench system of the 3-CRU is thus a constant. That is to say, the 3-CRU translational parallel manipulator is free from constraint singularity.

3.5.2 Kinematic Singularities

When type II kinematic singularity occurs for a parallel manipulator, the moving platform can undergo infinitesimal or finite motion when the inputs are specified. It will be proved below that, there is no type II singularity for the 3-CRU translational parallel manipulator.

From Section 3.5.1, it is known that no rotation singularity exists for the 3-CRU translational parallel manipulator. Thus, equation (3.19) is always satisfied. Uncertainty singularities for the 3-CRU translational parallel manipulator occur if and only if \mathbf{J} is singular.

From Section 3.4, it is known that the Jacobian matrix, \mathbf{J} , is an identity matrix. Thus, no type II singularity exists for the 3-CRU translational parallel manipulator.

3.6 Stiffness Analysis

3.6.1 Introduction

Compare with serial manipulators, parallel manipulators offer an improved stiffness and better accuracy. This feature makes them attractive for innovative machine tool structures for high speed machining [37, 38, 39].

The stiffness properties of a manipulator can be defined through a 6×6 matrix that is called stiffness matrix K .

Several methods exist for the computation of the stiffness matrix: the Finite Element Analysis (FEA) [40], the matrix structural analysis (SMA) [41], and the virtual joint method (VJM) which is also called the lumped modeling [42, 43].

The FEA is proved to be the most accurate and reliable; however, this method has the disadvantage that it requires an extensive computation time [44]. The SMA also incorporates the main ideas of the FEA, but operates with rather large elements, 3D flexible beams describing the manipulator structure. This leads obviously to the reduction of the computational expenses, but does not provide clear physical relations required for the parametric stiffness analysis. Finally, the VJM method is based on the expansion of the traditional rigid model by adding the virtual joints, which describe the elastic deformations of the links.

3.6.2 General Stiffness Model for Parallel Manipulator

As introduced in Section 3.6.1, there are three methods to build mechanism stiffness models. Among them, the method that relies on the calculation of the parallel mechanism's Jacobian matrix is adopted in this thesis [42, 43].

The stiffness of a parallel mechanism is dependent on the joint's stiffness, the legs structure and material, the platform and base stiffness, the geometry of the structure, the topology of the structure and the end-effector position and orientation.

The stiffness of a parallel mechanism at a given point of its workspace can be characterized by its stiffness matrix. This matrix relates the forces and torques applied at the gripper link in Cartesian space to the corresponding linear and angular Cartesian displacement. It can be obtained using kinematic and static equations.

Note, that link stiffness is not considered in conventional joint stiffness analysis approach. That means links of the mechanism are assumed strictly rigid.

The joint displacement, Δq , is related to the end-effector displacement in Cartesian space Δr , by the conventional Jacobian matrix \mathbf{J} ,

$$\Delta q = \mathbf{J} \Delta r \quad (3.22)$$

Under the principle of virtual work, the end-effector force F in terms of the actuated joint torques τ is given as the following:

$$F = \mathbf{J}^T \tau \quad (3.23)$$

Then τ can be related to Δq by a diagonal actuated joint stiffness matrix $\mathbf{K}_j = \text{diag}[k_1, \dots, k_n]$, whose elements k_i are the stiffness of each actuator, as follow:

$$\tau = \mathbf{K}_j \Delta q \quad (3.24)$$

Substituting equation (3.22) into equation (3.24) and the resulting equation into equation (3.23), then we have:

$$F = \mathbf{J}^T \mathbf{K}_j \mathbf{J} \Delta r \quad (3.25)$$

Therefore, the stiffness matrix of a parallel manipulator is given by:

$$\mathbf{K}_r = \mathbf{J}^T \mathbf{K}_j \mathbf{J} \quad (3.26)$$

Particularly, in the case for which all the actuators have the same stiffness, i.e., $k_1 = k_2 = \dots = k_n$, then equation (3.26) will be simplified to:

$$\mathbf{K} = k \mathbf{J}^T \mathbf{J} \quad (3.27)$$

which is the equation given in [42]

3.6.3 Stiffness Mapping

As introduced in Section 3.4, \mathbf{J} is a 3 x 3 identity matrix, so we have $\mathbf{J}^T \mathbf{J} = 1$, the stiffness matrix of this 3-CRU manipulator is

$$\mathbf{K} = k \quad (3.28)$$

The above model is now used to obtain the stiffness maps for this 3-DOF decoupled parallel manipulator. A program has been written with the software Matlab. Given the value in Tables 3.1 to 3.3, the stiffness mesh graphs in X, Y, Z are shown in Figures 3.2 to 3.4.

From the stiffness mesh graphs in X (Figure 3.2), Y (Figure 3.3), and Z (Figure 3.4), one can conclude that the stiffness in X, Y, and Z will not change while the position and orientation are changing. That means the stiffness of the actuators is the main factor

to determine the stiffness in the situations. The results also indicate that the stiffness is a constant within its workspace; this will improve the kinematic accuracy.

As a result, the desired stiffness on X, Y, and Z directions can be achieved by adjusting the stiffness of the actuators. Moreover, when using this 3-DOF parallel manipulator for parts assembly or as a machine tool, one can judge if the parallel manipulator is stronger enough to perform the tasks by considering the workloads in X, Y, and Z directions.

Table 3.1 Stiffness in X vs. Stiffness to actuators

K N/m	k N/m
500	500

Table 3.2 Stiffness in Y vs. Stiffness of actuators

K N/m	k N/m
500	500

Table 3.3 Stiffness in Z vs. Stiffness of actuators

K N/m	k N/m
500	500

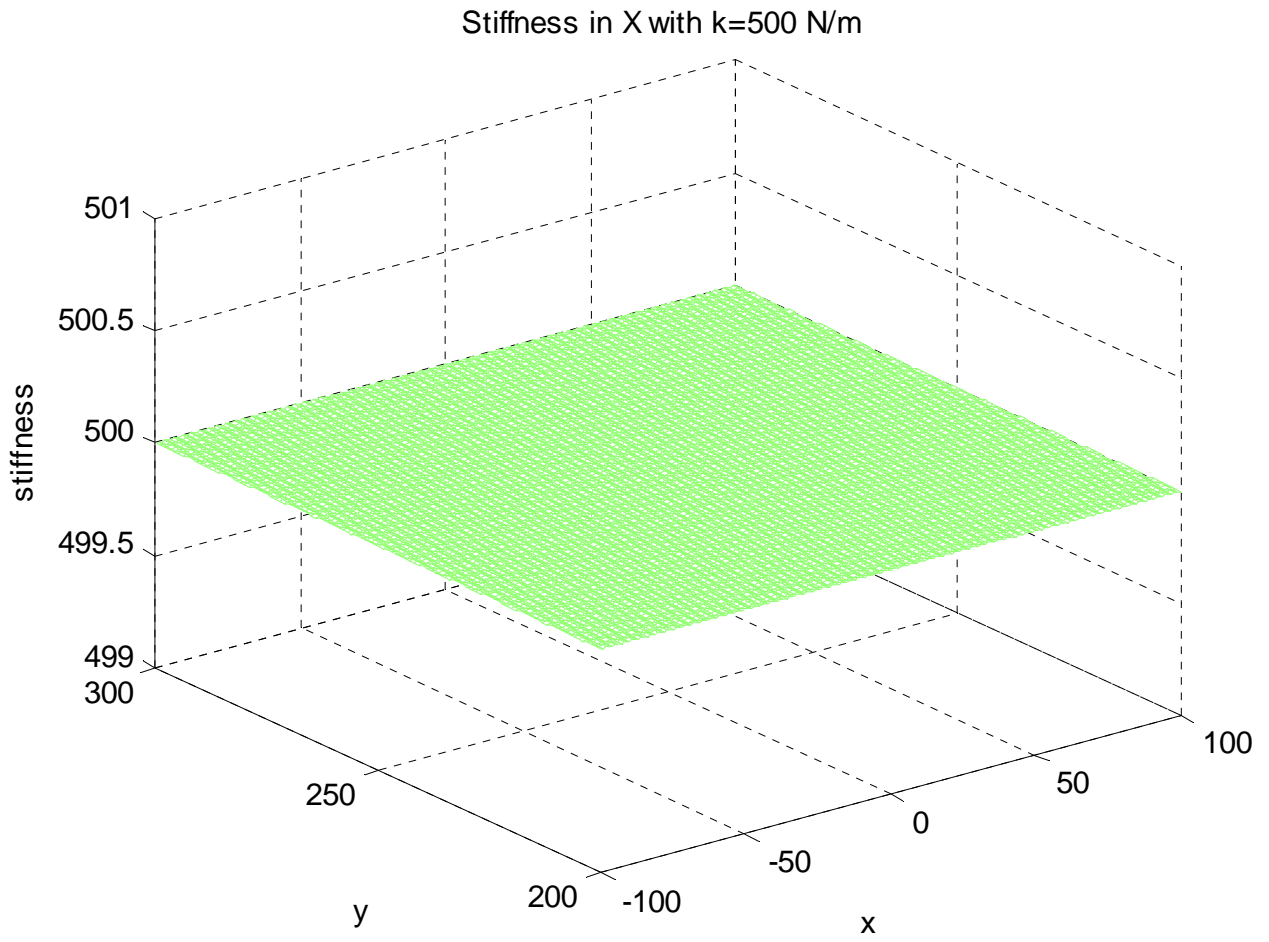


Figure 3.2 Stiffness mesh graphs in X with $k = 500$ N/m

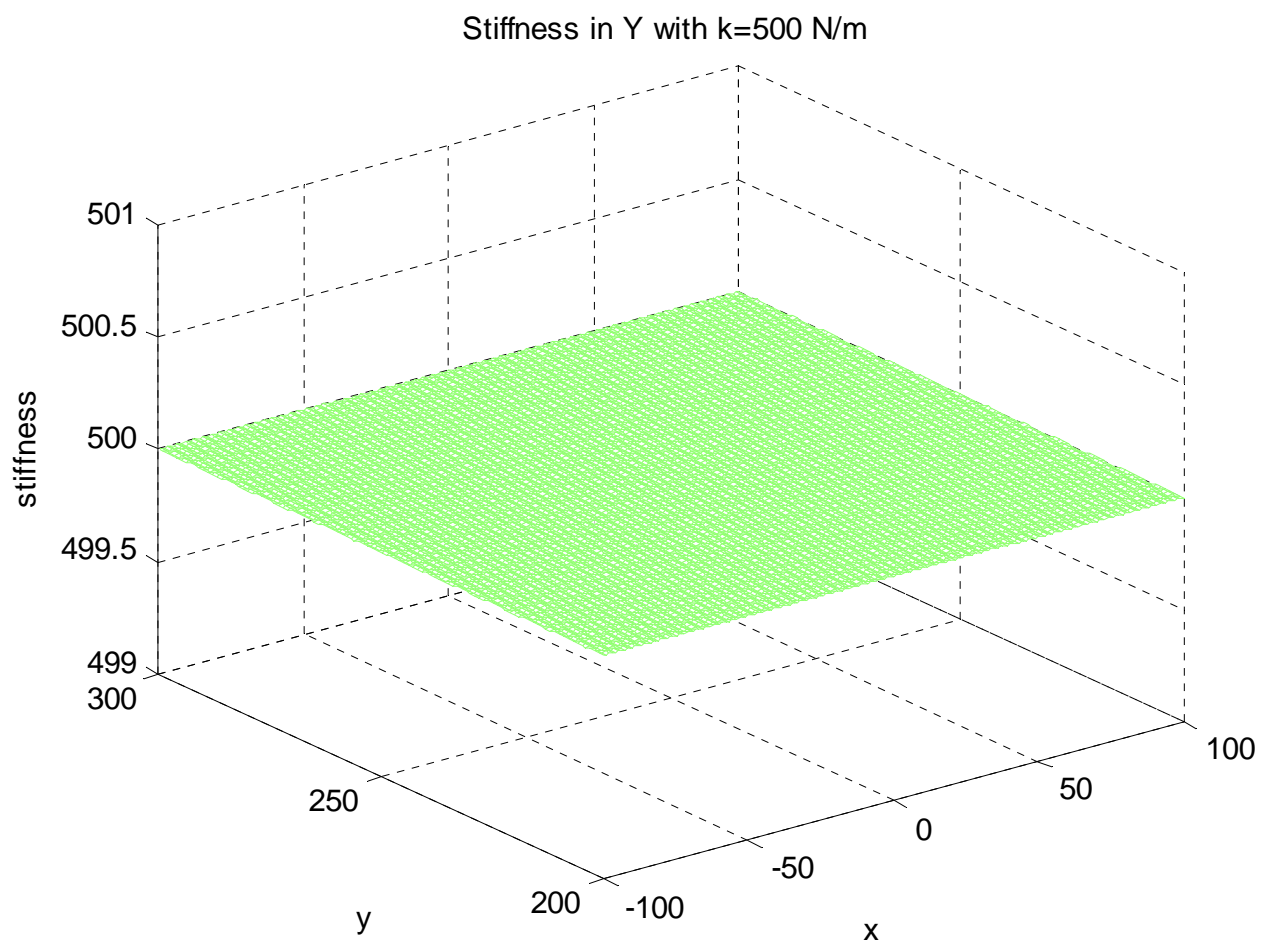


Figure 3.3 Stiffness mesh graphs in Y with $k = 500$ N/m

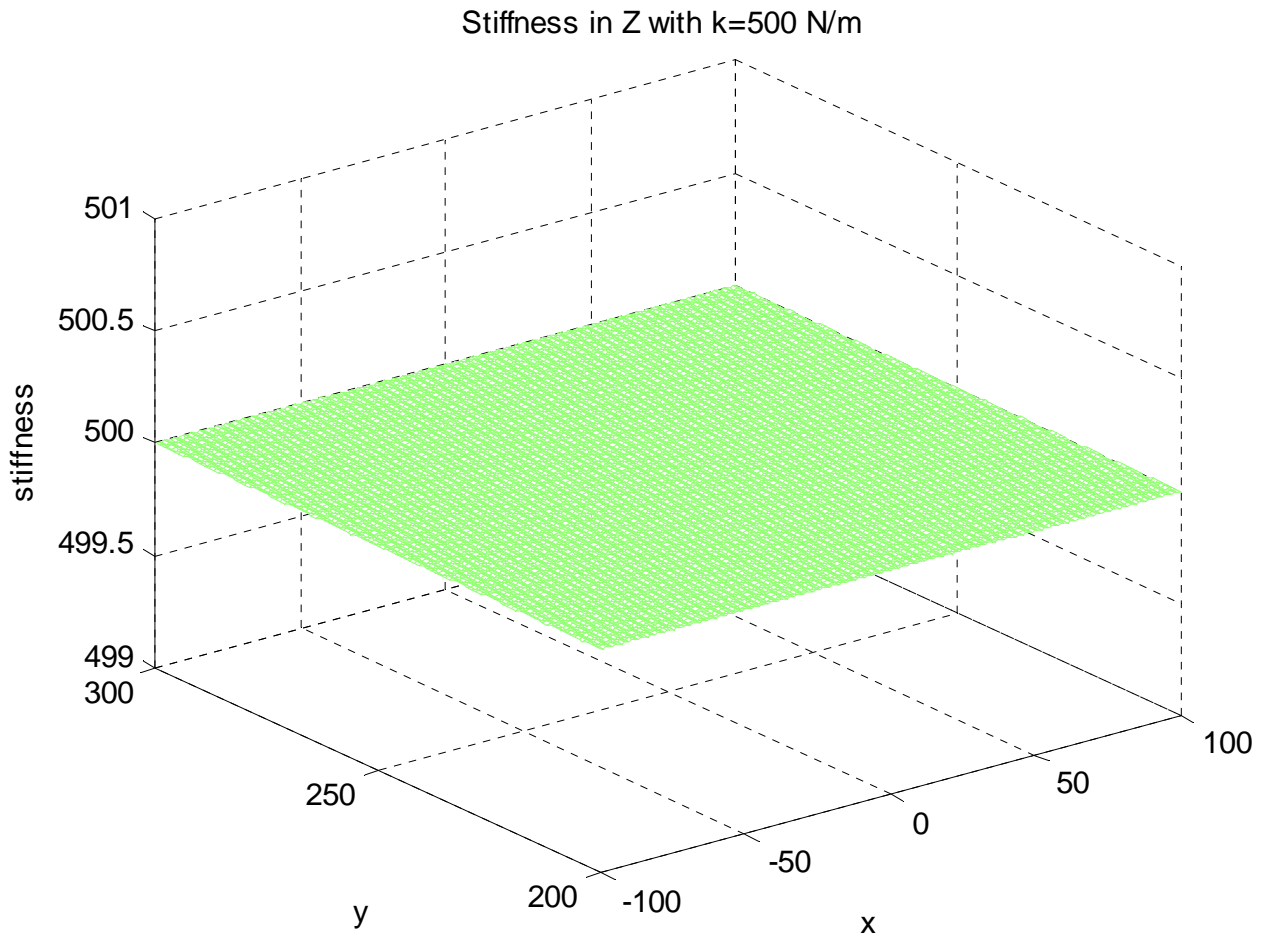


Figure 3.4 Stiffness Mesh Graphs in Z When $k = 500$ N/m

Chapter 4

Workspace Analysis and Prototype Design

4.1 Definition of the Workspace

The workspace of the Parallel robot can be defined as a reachable region of the origin of a coordinate system attached to the center of the moving plate. Since its major drawback is a limited workspace, it is of primary importance to develop algorithms by which the workspace can be determined and the effect of different designs on the workspace can be evaluated.

There are several types of workspace [6]:

- Constant orientation workspace or translation workspace
- Orientation workspace
- Maximal workspace or reachable workspace
- Inclusive orientation workspace
- Total orientation workspace
- Dextrous workspace
- Reduced total orientation workspace

Various approaches may be used to calculate the workspace of a parallel manipulator, such as geometrical approach, discretisation method, and numerical methods [6].

The most common one is the geometrical approach. The purpose of this approach is to determine the boundary of the robot workspace geometrically.

4.2 Workspace Analysis of the 3-CRU Parallel Manipulator

From equations (3.15) to (3.17), it appears clearly that the Cartesian workspace consists of a parallelepiped. A regular workspace (parallelepiped) is very attractive in practice.

Since we use linear actuators for the 3-CRU parallel manipulator, the workspace is limited by the stroke lengths d_i . However, it is preferable to make the links of length l_{1i} and l_{2i} sufficiently long to ensure that additional constraints are not imposed on the mechanism, so that the ranges of motion of all linear actuators can be fully utilized. To implement this, we applied the constraint that the workspace volume is always equal to the product of the stroke lengths of the linear actuators.

Finally, we obtain the workspace of the parallel manipulator shown in Figure 4.1.

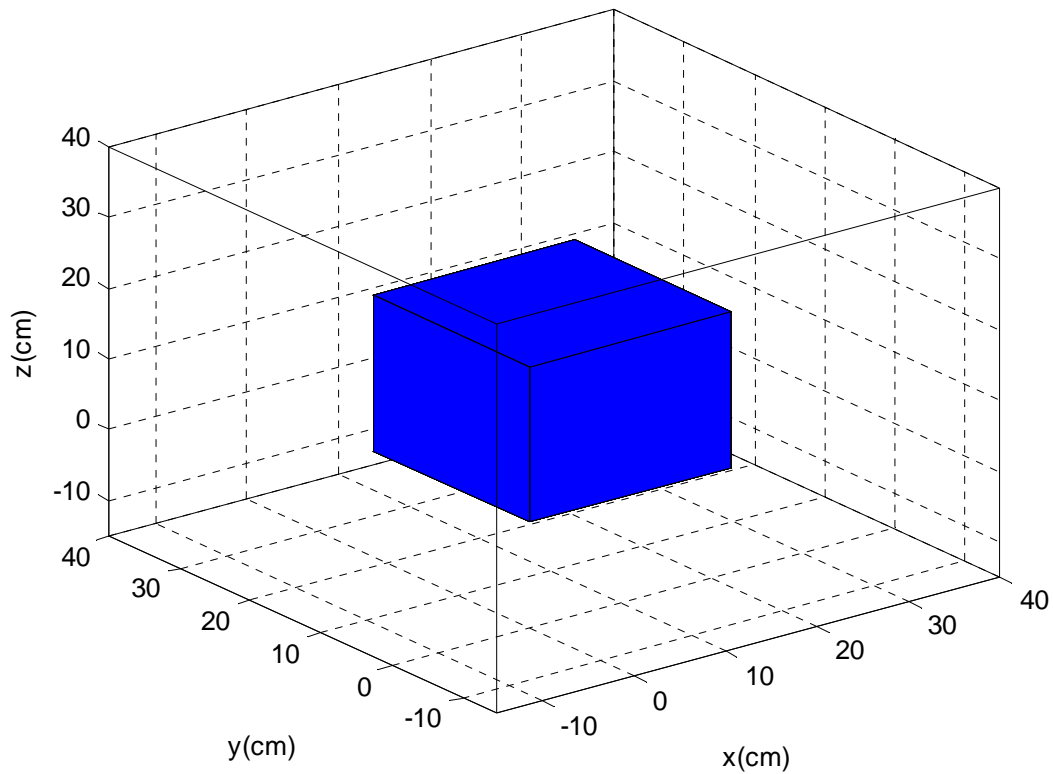


Figure 4.1 Workspace

4.3 Prototype Design

Based on the 3-CRU architecture described in Chapter two, we focus on the prototype design of the manipulator in this section.

The key issues in the detailed design of the 3-CRU translational parallel manipulator are described as follows:

1. Adopt linear actuation layout; a linear actuator drives the C joint in each leg (see Figure 2.1 for detail), whereas all the other joints are passive. One of the advantages is to

have all actuators installed on the fixed base. The C joints will be driven using toothed belts connected to DC servomotors.

2. The selection of the assembly modes of each leg

In selecting the assembly modes of each leg, the location of the work piece to be placed should be taken into consideration.

For the 3-CRU translational parallel manipulator, the work piece is placed under the moving platform.

3. The determination of the link lengths of l_{1i} and l_{2i}

In determining the link lengths l_{1i} and l_{2i} , the issue of avoiding link interferences should be taken into consideration.

To address this issue, l_{1i} and l_{2i} are adjusted to avoid interference among links in the three legs and the moving platform by simulating the motion of the parallel manipulator using a CAD software.

Consider the requirements of feasibility concerning dimensional limits for manufacturing parts, encoders available in the market, and the need for a continuous working space with no interference of moving parts, the following choices for the geometric parameters of the 3-CRU manipulator (see Figure 3.1 for d , l , b , and m):

Stroke length: $d_1 = d_2 = d_3 = 220$ mm

Length of leg: $l_{1i} = l_{2i} = 325$ mm

Dimension of the moving plate: $b = 30$ mm

The distance between the center of the moving plate and base: $m = l_{2i} + b = 355$ mm

Chapter 5

Design Optimization

5.1 Introduction

Optimization is to find the best solution for a problem under given circumstance. Mathematical optimization means that the problem at hand is formalized in a stringent mathematical way and the best solution under the given circumstances is found by using mathematical algorithms. When it comes to design optimization, Papalambros et al. give the following definition in [45]:

Informally, but rigorously, we can say that design optimization involves:

1. The selection of a set of variables to describe the design alternatives.
2. The selection of an objective (criterion), expressed in terms of the design variables, which we seek to minimize or maximize.
3. The determination of a set of constraints, expressed in terms of the design variables, which must be satisfied by an acceptable design.
4. The determination of a set of values for the design variables, which minimize (or maximize) the objective, while satisfying all the constraints.

There are many different optimization algorithms used in engineering design. The algorithms can be divided into gradient-based and non gradient-based methods. The gradient-based methods have been thoroughly studied and a considerable body of literature is available on the subject [46-48]. The gradient- based methods are suitable for problems with continuous variables and differentiable functions since they operate with gradients of the problem functions.

Direct search methods are one example of algorithms, which do not calculate derivatives. Examples of direct search methods include the Nelder-Mead simplex method [49], Box's Complex method [50], the Hooke and Jeeves pattern search [51], and the Dennis and Torczon parallel direct search algorithm (PDS) [52]. A thorough review of direct search methods can be found in [53]. Other non-gradient methods are stochastic methods such as Genetic algorithms (GA) [54] are comprehensively studied in [55]. Simulated annealing was developed by Kirkpatrick [56] in the early 1980s. More recent methods include Tabu search, developed by Glover [57], response surface approximations [58], Taguchi methods [59], and Particle Swarm (PS) [60].

5.2 Genetic Algorithms

Genetic algorithm (GA) is a search algorithm based on the hypothesis of natural selection and genetics. In the methods, each optimization variable is encoded by a gene using an appropriate representation. The corresponding genes for all parameters form a chromosome (or point) capable of describing an individual design solution. A finite

length string, such as a binary string of zeros and ones, is usually used to represent each chromosome.

Today real value chromosomes are common, whereas original GAs used binary representations of the optimization variables. A set of alternative points (called population) at an iteration (called generation) is used to generate a new set of points. In this process, combinations of the most desirable characteristics of the current members (individuals) of the population are used to generate new populations better than the current ones. When comparing different points the term fitness is used. Fitness is defined using the objective function or the penalty function for constrained problems. The fitness value is calculated for each member of the population, such that the fittest individuals are the ones with the highest likelihood of survival.

The Genetic Algorithm starts with a set of randomly generated individuals (points). Three operators are then needed to implement the algorithm: (i) selection; (ii) crossover; and (iii) mutation. Selection is an operator where an old string (point) is copied into the new population according to its fitness. Individuals with higher fitness are more likely to produce offspring. The crossover operator corresponds to allowing the selected individuals to exchange characteristics among themselves. Crossover entails selection of starting and ending positions on a pair of mating strings at random and simply exchanging the strings of zeros and ones between these positions. Mutation corresponds to selection of a few individuals of the population, determining a location on the string at random and switching the 0 to 1 or vice versa. The foregoing three steps are repeated for successive generations of the population until no further improvement in the fitness is

possible, or the number of generation reaches a specified limit. The individual in this last generation with the best fitness value is taken as the optimum.

5.3 The Optimum Design for the 3-CRU Manipulator with Prescribed Workspace

Parallel mechanisms create great interest because they can be used for many applications in industrial such as machine tools or light assembly.

Obtaining high performance requires the choice of suitable mechanism dimensions especially as there is much larger variation in the performances of parallel architectures according to the dimensions than for classical serial ones. Indeed, with the development of manipulators for performing a wide range of tasks, the introduction of performance indices or criteria, which are used to characterize the manipulator, has become very important. A number of different optimization criteria for manipulators may be appropriate depending on the resources and general nature of tasks to be performed. The choice of any of the criteria for a given set of data would result in a manipulator whose performances do not necessarily match the optimum values of the other criteria.

Workspace is one of the most important properties because workspace determines geometrical limits on the task that can be performed. Most of the done works are related to maximize the position workspace [66], or to try to obtain a position workspace as close as possible to a prescribed one [67-68].

In this thesis, we will optimize the design of the 3-CRU architecture with its position workspace is suitably prescribed. The approach presented in [69] will be adopted and GA is applied. The flow chart in Figure 5.1 shows the sequence of the basic operators used in genetic algorithms.

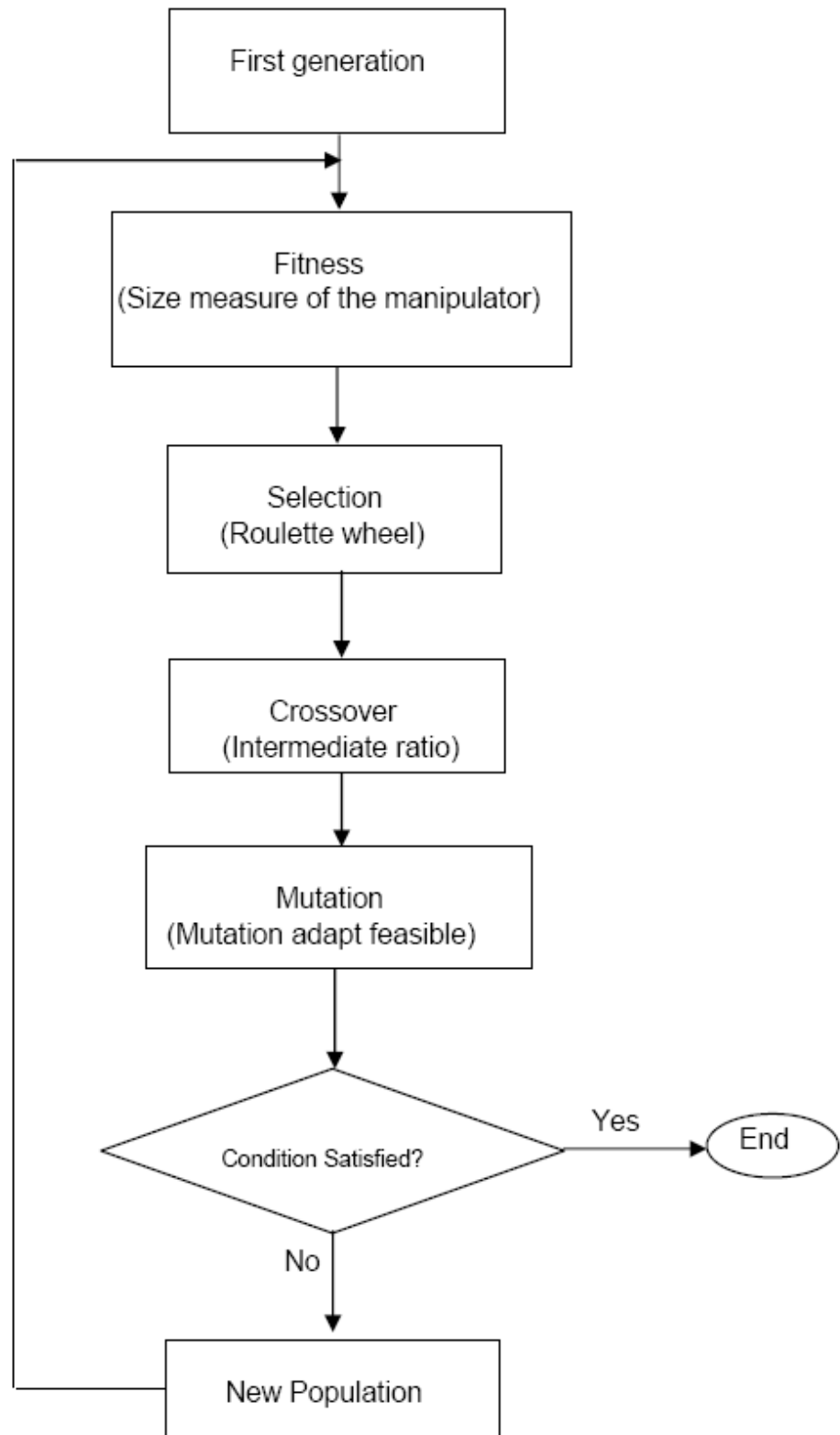


Figure 5.1 Genetic algorithm flow chart

The optimum design problem for the 3-CRU architecture can be formulated as:

$$\text{Objective function } L = l_{1i}^2 + l_{2i}^2 + b^2 \quad (i = 1,2,3) \quad (5.1)$$

where L denotes the size measure of the manipulator.

$$\text{We assume that } l_{11} = l_{12} = l_{13}, l_{21} = l_{22} = l_{23}$$

In order to complete the design characterization and use prescribed data, the optimization problem is also subject to constraints from the position point of view:

$$\begin{aligned} X_{\max} &\leq X'_{\max} \\ Y_{\max} &\leq Y'_{\max} \\ Z_{\max} &\leq Z'_{\max} \end{aligned} \quad (5.2)$$

where the left-hand values correspond to the orientation volume W_L^* and the prime values describe the prescribed parallelepiped W_L

Summarizing the optimum design for the 3-CRU architecture has been formulated by equations (5.1) to (5.2) and the W_L by taking into account only workspace characteristics to give the smallest manipulator fitting the prescribed workspaces. Here the prescribed workspace is the one we have in chapter 4, which is 0.0106 m^3 .

In addition, the forward kinematics presented in equations (3.15) to (3.17) is useful and computationally efficient to determine extreme reaches of equation (5.2).

The number of variables is to be determined. In this design, they are b, l_{11} and l_{21} .

So the vector of optimization variables is therefore:

$$\mathbf{a} = [l_{11}, l_{21}, b] \quad (5.3)$$

and their bounds are:

$$l_{11} \in [300,350], l_{21} \in [300,350], b \in [30,50] \text{ mm}$$

The population size and the generation number have to be selected. The generation number is the maximum number of iterations the GA performs and the population size specifies how many individuals there are in each generation. In this case, the population size is set to 10; the maximum generation number is 100.

The Figure 5.2 displays a plot of the best and mean values of the fitness function at each generation.

The following figure also displays the best and mean values in the current generation numerically at the top of the figure.

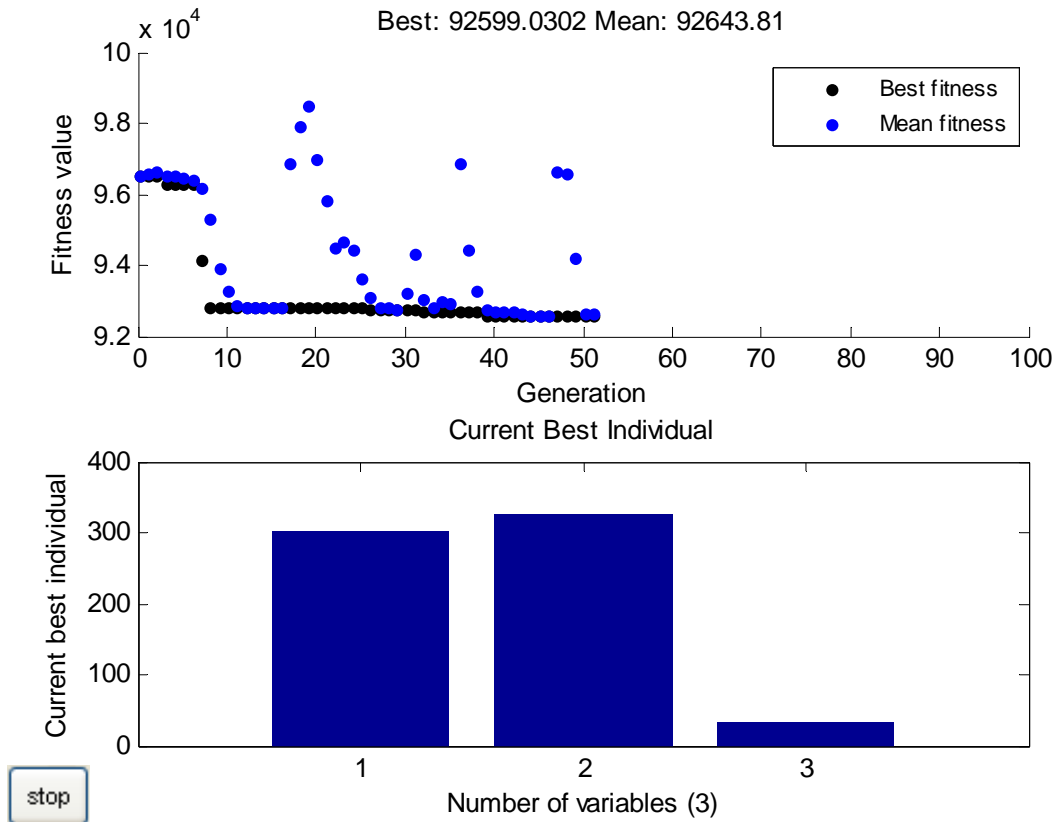


Figure 5.2 The best fitness and the best individuals of the design optimization

The optimal parameters are obtained after 51 generations as follows:

$$\mathbf{a} = [l_{11}, l_{21}, b] = [302.50511, 324.9706, 33.01029]$$

which suggest the optimal design values for the length of links of the leg and the dimension of the end-effector are:

$$d = l_{11} = 302.51\text{mm}, l_{21} = 324.97\text{mm}, b = 33.51\text{mm}$$

Table 5.1 below shows the original design parameters and optimum design parameters of the 3-CRU parallel manipulator with the same workspace.

Table 5.1 Original design parameters and optimum design parameters

	l_{11} (mm)	l_{21} (mm)	b (mm)	Workspace (m ³)
Original design	325	325	30	0.0106
Optimum design	302.51	324.97	33.51	0.0106

Chapter 6

Conclusions and Future Research

6.1 Conclusions

In this thesis, a study has been presented on the design of a translational parallel manipulator with decoupled motions.

The parallel manipulator has 3-DOF, and can be used for parts assembly and light machining tasks that require large workspace, high dexterity, high loading capacity, and considerable stiffness.

In chapter 1, an overview of the history of robots was presented. The research on 3-DOF parallel manipulators has been leaning toward the decoupling of the position and orientation of the end-effector. Therefore, this thesis set out to design a novel 3-DOF non-over-constraints translational parallel manipulator with decoupled motions.

The classifications of kinematic decoupling, isotropy and constitution principal for parallel manipulators as well as screw theory have been studied in chapter 2. In this chapter, we focus on the conceptual of the new design, and a novel 3-DOF non-over-constraint translational parallel manipulator with decoupled motion has been proposed. The screw theory has been adopted for the mobility analysis of the parallel manipulator.

In chapter 3, kinematic modeling of the new parallel manipulator has been examined, in terms of inverse and forward kinematics study, velocity analysis, singularity

analysis, as well as stiffness analysis. It has been noticed that due to the isotropy and motion decoupling, the inverse and forward kinematic are easy for analysis; The Jacobian is a 3 x 3 identity matrix; and the kinematic accuracy can be well improved, as the stiffness is a constant within the parallel manipulator's workspace.

The geometrical method was selected to determine the workspace of the parallel manipulator in chapter 4. The workspace simulation graphically describes all the locations of operation points, which the end-effector can reach, which is very useful to define the reach ability of the parallel manipulator. In this chapter, some of the key issues in the detailed prototype design of the 3-CRU manipulator were discussed as well. Geometric parameters of the manipulator have been given for further work.

GA has been adopted in chapter 5 to optimize the design parameters of the manipulator with suitable prescribed workspace.

6.2 Major Contributions

The major contribution of this thesis is to have proposed a novel 3-DOF parallel manipulator with features such as lower mobility, decoupled motions, and isotropic. These advantages have great potential for machine tools and Coordinate Measuring Machine.

6.3 Future Research

The following issues may deserve more attentions in the future.

- To build prototype of this design
- To conduct kinematics calibration and error compensation study
- To perform a comprehensive study of new parallel manipulator with kinematic decoupling of great potential application. The comprehensive study will include the constraint singularity analysis, the forward kinematics, the inverse kinematics, the kinematic error analysis, the workspace analysis and the kinematic design.
- To investigate other practical applications, such as a parallel module with kinematic decoupling of a hybrid machine tool.

References:

- [1]. Vitruvius, M., Vitruvius: ten books on architecture/translation [from the Latin] by Ingrid D Rowland; commentary and illustrations by Thomas Noble Howe; with additional commentary by Ingrid D Rowland and Michalel Dewar, ed. I D Rowland, T N Hown, and M J Dewar. 1999, Cambridge; New York: Cambridge University Press. xvi, 333 p: ill; 28 cm
- [2]. Pollard, W.L.V., "Position controlling apparatus," US Patent No. 2,286,571, June 16, 1942
- [3]. Gough, V.E. and Whitehall, S.G., "Universal Tyre Test Machine." Proceedings of the F.I.S.I.T.A. Ninth International Technical Congress, pp 117-137, T May 1962,
- [4]. Stewart, D., "A platform with six degrees of freedom". Proceedings of the IMechE, Vol. 180, Pt. 1, No. 15, pp. 371-385, 1965-
- [5]. Clavel, R. "Device for the movement and positioning of an element in space". US Patent No. 4,976,582, December 11, 1990.
- [6]. Merlet, J.P., "Parallel Robots", 2nd Edition, Springer, 2006
- [7]. Gosselin, Cl., Hamel, J.-F., " The agile eye: a high-performance three-degree-of freedom camera-orienting device". In IEEE International Conference on Robotics and Automation, pages 781–786, San Diego, California, USA, 1994.
- [8]. Chablat, D., Wenger, Ph., "Working Modes and Aspects in Fully Parallel Manipulators," IEEE International Conference on *Robotics and Automation*, pp.1964-1969, 1998.
- [9]. Arai, T., Cleary, K., Homma, K., Adachi, H. and Nakamura, T., "Development of parallel link manipulator for underground excavation task",

Proceedings of 1991 International Symposium on Advanced Robot Technology,
pp. 541-548.

- [10]. Gosselin, C. and Angeles, J., "The optimum kinematic design of a planar
Three-degree-of-freedom parallel manipulator", ASME J. Mechanical
Transmission, Automation and Design, Vol. 110, pp. 35-41.
- [11]. Waldron, K.J., Vohnout, V.J., Pery, A., McGhee, R.B., "Configuration Design of
the Adaptive Suspension Vehicle", International Journal of Robotics Research,
Summer 1984
- [12]. Hunt, K.H., "Kinematic Geometry of Mechanisms", Clarendon Press, Oxford,
1978
- [13]. Giddings and Lewis, "Giddings and Lewis Automation technology," Fond Du
Lac, WI, 1996
- [14]. Aronson, R. B., "A bright horizon for machine tool technology," *Manuf. Eng.*, pp.
57-70, 1996
- [15]. Grigore, G., Structural synthesis of fully-isotropic translational parallel robots
via theory of linear transformations, *European Journal of Mechanics A/Solids* 23
(2004) 1021–1039
- [16]. Lee, K. M., Shah, D. K., "Kinematic Analysis of A Three-degree-of-Freedom In-
Parallel Actuated Manipulator", *IEEE J. of robotics and Automation*, 1988, Vol.4,
No.3, 354-360
- [17]. Clavel, R., "Delat, A Fast Robot with Parallel Geometry", *Proceedings of the 18th
Int. Symp. On Industrial Robots*, 1988, Vol.1, 91-100
- [18]. Wang, J., Gosselin, C. M., "Kinematic Analysis and Singularity Loci of

- Spatial Four-Degree-of-Freedom Parallel Manipulators Using A Vector Formulation”, ASME J. of Mechanical Design, 1998, Vol.120, 555-558
- [19]. Wang, J., Gosselin, C. M., “Kinematic Analysis and Singularity Representation of Spatial Five-Degree-of-Freedom Parallel Manipulators”, Int. J. of Robotic System, 1997, Vol.14, 851-869 mechanical Design, 1998, Vol.120, 555-558
- [20]. Tsai, L. W., 1999, “Then Enumeration of a Class of Three-DOF Parallel Manipulators,” 10th World Congress on the Theory of Machine and Mechanisms Olulu, Finland, June 20-24, 3, pp. 1121-1126
- [21]. Zhang, D., Bi, Z., “Development of Reconfigurable Paralel Kinematic Machines using Modular Design Approach”.
- [22]. Tsai, L.W., Walsh, G.C., Stamper, R., “Kinematics of a Novel Three DOF Translational Platform,” Proc. of the 1996 IEEE International Conference on Robotics and Automation, Minneapolis, MN, 3446-3451 (1996).
- [23]. Tsai, L.W., “Kinematics of a Three-DOF Platform Manipulator with Three Extensible Limbs,” in Recent Advances in Robot Kinematics, Edited by J. Lenarcic and V. Parenti-Castelli, Kluwer Academic Publishers, London, 401-410 (1996).
- [24]. Kim, H. S., Tsai, L.W., “Design Optimization of a Cartesian Parallel Manipulator.” Journal of Mechanical Design 125 (1) (2003) 43-51
- [25]. Zhao, T.S., Huang, Z., “A Novel Three-DOF Translational Platform Mechanism and Its Kinematics,” Proc. of the 2000 ASME Design Engineering Technical Conferences, Baltimore, MD, MECH-14101(2000)
- [26]. Kong, X.W., Gosselin, C. “Kinematios and singularity analysis of a novel type of

3-CRR 3-DOF translational parallel manipulator”, International Journal of Robotic Research 21 (9) (2002) 791-798

- [27]. Yang, T.L., and Yao, F.H., “The Topological Characteristics and Automatic Generation of Structural Analysis and Synthesis of Plane Mechanisms, Part 1: Theory; Part 2: Application,” Proceedings of ASME Mech. Conf., Vol 15 (1), pp. 179-190. , 1988
- [28]. Yang, T.L., Yao, F.H., “Topological Characteristics and Automatic Generation of Structural Analysis of Spatial Mechanism, Part 1: Topological Characteristics of Mechanical Networks; Part 2: Automatic Generation of Structural Types of Kinematic Chains,” Proceedings of SAME Mech. Conf., Phoenix, DE-47, pp.179-190, 1992
- [29]. Meng, J., an Li,Z., “A general approach for accuracy analysis of parallel manipulators with joint clearance,” in Proceeding of IEEE/RSJ International Conference on Intelligent Robots and Systems, (Edmonton, Alberta, Canada), pp 790-795, Aug.2-6,2005
- [30]. Tsai, L.W., “Robot Analysis: The Mechanisc o Serial and Parallel Manipulators.”, Wiley, New York, 1999
- [31]. Kong, Xianwan, Gosselin, C., “A Class of 3-DOF Translational Parallel Manipulators with Linear Input-Output Equations.” Proceedings of the workshop on Fundamental Issues and future Research Directions for Parallel Mechanisms and Manipulators, October 3-4,2002, Quebec City, Quebec, Canada
- [32]. Ball, R.S., “A Treatise on the Theory of Screws”, Cambridge Mathematical Library, 1876

- [33]. Hunt, K.H., Kinematic Geometry of Mechanisms. Oxford University Press, 1978
- [34]. Salisbury, J.K., Craig, J.J., "Articulated joint: force and kinematic issue", Int. J. of Robotics Research, vol. 1(1), pp.1-17,1982
- [35]. Angeles, J., "Fundamentals of Robotic Mechanical Systems: Theory, Methods, and Algorithms", New York: Springer, 1987
- [36]. Fattah, A., Hasan Ghasemi, A.M., "Isotropic design of spatial parallel manipulators", Int J. of Robotics Research, vol. 21(9), pp. 811-824, 2002
- [37]. Tlustý, J. Z., Ridgeway, S., "Fundamental Comparison of the Use of Serial and Parallel Kinematics for Machine Tools", Annals of the CIRP, vol. 48(1), 1999.
- [38]. Wenger, P., Gosselin, C.M., and Maille, M, "A Comparison study of Serial and Parallel", Mechanism Topologies for Machine Tools, PKM'99, pp.23-32, Milano, 1999
- [39]. Majou, F., Wenger, P., and Chablat, D., "The design of Parallel Kinematic Machine Tools using Kinestatic Performance Criteria", 3rd International Conference on Metal Cutting and High Speed Machining, Metz, France, June 2001
- [40]. Majou, F., Gosselin, C., Wenger, P., and Chablat, D., "Parametric stiffness analysis of the orthoglide", Mechanism and Machine Theory, vol. 42(3), pp. 296-311, March 2007
- [41]. Bouzgarrou, B.C., Fauroux, J.C., Gogu, G., and Heerah, Y., "rigidity analysis of T3R1 parallel robot uncoupled kinematics", Proc. Of the 35th International Symposium on Robotics (ISR), Paris, France, March 2004

- [42]. Gosselin, C.M., “Stiffness mapping for parallel manipulators”, IEEE transactions on Robotics and Automation, vol.6, pp.377-382,1990
- [43]. Gosselin, C.M., and Zhang, D., “Stiffness Analysis of Parallel Mechanisms Using a Lumped Model”, International Journal of Robotics and Automation, vol. 17, No.1 2002
- [44]. Company, O., Pierrot, F., “Modeling and design issues of a 3-axis parallel machine-tool, Mechanism and Machine theory, 37, 2002, 1325-1345
- [45]. Papalambros Y. P. and Wilde J. D., Principles of Optimal Design – Modeling and Computation, Cambridge University Press, 1988.
- [46]. Nash S. and Sofer A., “Linear and nonlinear programming”, McGraw-Hill, 1996.
- [47]. Nocedal J. and Wright S. J., “Numerical optimization”, Springer-Verlag, 2006.
- [48]. Ruszczyński A., “Nonlinear optimization”, Princeton University Press, 2006.
- [49]. Nelder J.A. and Mead R., “A simplex method for function minimization”, Computer Journal, Vol. 7, pp. 303-313, 1965.
- [50]. Box M. J., “A new method of constrained optimization and a comparison with other methods”, Computer Journal, 8:42-52, 1965.
- [51]. Hooke R. and Jeeves T. A., “Direct search solution of numerical and statistical problem”, Journal of the Association for Computing Machinery, Vol. 8, pp. 212- 229, 1961.
- [52]. Dennis J. E. and Torczon V., “Direct search methods on parallel machines”, SIAM Journal of Optimization, Vol. 1, pp. 448-474, 1991.
- [53]. Kolda G.T., Lewis R.M. and Torczon V., “Optimization by Direct Search :New

- Perspectives on Some, Classical and Modern Methods”, SIAM REVIEW, Vol. 45, No. 3, pp. 385–482, Society for Industrial and Applied Mathematics, 2003.
- [54]. Holland J. H., “Adaption in Natural and Artificial System”, University of Michigan Press, Ann Arbor, 1975.
- [55]. Goldberg D. E., “Genetic Algorithms in Search and Machine Learning”, Addison Wesley, Reading, 1989.
- [56]. Kirkpatrick S., Gelatt C. D., and Vecchi M. P., “Optimization by simulated annealing,” Science, Vol. 220, pp. 671-680, 1983.
- [57]. Glover F., “Tabu Search - Part I, ORSA Journal on Computing”, Vol. 1, pp. 190- 206, 1989.
- [58]. Marvis D. and Qiu S., “An Improved Process for the Generation of Drag Polars for use in Conceptual/Preliminary Design”, in Proceedings of SAE World Aviation Conference, San Francisco, USA, October 19-21,1999.
- [59]. Connor A. M., “Parameter Sizing for Fluid Power Circuits Using Taguchi Methods”, Journal of Engineering Design, Vol. 10, No. 4, 1999.
- [60]. Kennedy J. and Eberhart R., Particle swarm optimization, in Proceedings of the IEEE International Conference on Neural Networks, Piscataway, NJ, pp. 1942–1948, 1995.
- [61]. Ball, R. S., The Theory of Screws, Cambridge University Press, London, UK., 1990
- [62]. Wang, L., Xi., J., Smart Devices and Machines for Advanced Manufacturing Springer London, 2008
- [63]. Zlatanov, D., Bonev, I., Gosselin C.M., Constraint Singularities of Parallel

Mechanism, Proceedings of the 2002 IEEE International Conference on Robotics and Automation, Washington DC, May 2002, pp. 496-502

[64]. Gosselin, C.M., Angeles, J., Singularity Analysis of Closed-Loop Kinematic Chains, IEEE Trans. Rob. Autom., 6(3), pp. 281-290, 1990

[65]. Dietmaier, P. 1998. The Stewart–Gough platform of general geometry can have 40 real postures. *Proceedings of ARK*, Strobl, Austria, June 29–July 4, pp. 7–16.

[66]. Gosselin, C.M., Guillot, M., The Synthesis of Manipulators with Prescribed Workspace, Journal of Mechanical Design, Vol. 113, pp. 451-455, 1991

[67]. Boudreau, R., Gosselin, C.M., The Synthesis of Planar Parallel Manipulators with a Genetic Algorithm, Proceedings of the ASME Design Engineering Technical Conference, Atlanta, Paper DET2000/MECH-5957, 1998

[68]. Schonherr, J., Evaluation and Optimum Design of Parallel Manipulator Having a Defined Workspace, Proceeding of the ASME Design Engineering Technical Conference and Computers and Information in Engineering Conference, Baltimore, Paper DET/2000/MECH-14092, 2000

[69]. Laribi, M.A., Romdhane, L., Zegloul, S., Analysis and dimensional synthesis of the DELTA robot for a prescribed workspace, Mechanism and Machine Theory 42 (2007) 859 – 870